



## MODELING COMBUSTION CHEMISTRY IN LARGE EDDY SIMULATION OF TURBULENT FLAMES

**Benoît Fiorina, Denis Veynante, Sébastien Candel**

Ecole Centrale Paris  
CNRS, UPR 288, Laboratoire EM2C  
Grande Voie des Vignes  
92290 Châtenay-Malabry, France  
sebastien.candel@ecp.fr

### ABSTRACT

In addition to the complexities arising in non-reacting turbulent shear flows, the presence of highly exothermic chemical reactions introduces new difficulties. This central problem in combustion raises many fundamental issues with important practical applications. Progress in this field has been quite substantial. Advances on the theoretical level have been accompanied by significant developments in experimentation with laser diagnostics, high speed imaging and numerical data processing. Advances in computational combustion and more specifically in large eddy simulations have had a profound effect on scientific research in this field and on engineering applications. Starting with a brief tour of major issues in combustion, this article focuses on modeling strategies. The emphasis will be placed on modern approaches based on large eddy simulation. Issues related to a suitable description of chemistry and the possible use of tabulation methods will be specifically discussed and illustrated by examining selected topics of fundamental interest.

**Keywords :** *Turbulent combustion, Large eddy simulation, tabulated chemistry*

### INTRODUCTION

Combustion accounts for about 90 % of the global consumption of primary energy. Despite its environmental impact this share will probably not fall in the near future. Combustion delivers energy which is immediately available through the exothermic conversion of gaseous, liquid or solid fuels. There are no other ways to provide energy which are as convenient and as effective. In automotive or aerospace applications, combustion provides the required level of energy and the energy density of fuels is so large (about 40 MJ kg<sup>-1</sup> for standard hydrocarbon fuels) that it gives a considerable autonomy to the vehicle which cannot be matched by other means. While automobiles may run with electrical engines and batteries, it is less easy to replace current gas turbine engines by an electrical propulsion system in transport aircraft. The very high energy density which can be obtained from chemical conversion of reactants is also essential to rocket propulsion.

Production of electrical energy also heavily relies

on coal burning power plants and gas turbines (except in France where most of the electrical energy is derived from nuclear plants). One may think that the introduction of a greater amount of renewables like wind turbines or photovoltaics will reduce the need for fossil fuel powerplants. This is the case to some extent but renewable energy is essentially intermittent and wind turbines operate for about a quarter of the time. When production vanishes because of a lack of wind or sun and in the absence of massive capacities of electrical storage, the missing energy will have to be compensated. This is most readily accomplished by gas turbines which can be rapidly mobilized. It is interesting and somewhat paradoxical to note that the greater reliance on renewables will require at least on a short term additional capacities to produce power from fossil fuels. One may also note that in some emerging countries, the demand for energy is quite high and that this leads a country like China to open a new coal powerplant every week or so. Finally, it is important to keep in mind that there are many other applications of combustion in industrial processes, incineration and safety.

In addition to being a way of transforming energy combustion generates green house gases like CO<sub>2</sub>, and pollutants like carbon monoxide (CO), nitrogen oxides (NO<sub>x</sub>), unburned hydrocarbons (HC), soot and other chemical species that have an adverse effect on human health and the environment and need to be minimized. Environmental constraints and economic objectives drive a continuous search for more efficient combustion systems with reduced levels of pollutant emissions. Progress in this direction has been quite substantial with the simultaneous advances of a fundamental understanding of the basic mechanisms involved, enhanced diagnostics relying on lasers, optics and numerical imaging, improvements in experimental methodologies, developments in simulation software and high performance computing. Numerical modeling is now used on a routine basis in scientific research and engineering design. Because combustion raises many complex issues, there is no unique modeling method. While simple flames can be calculated by taking into account large kinetic schemes involving a few hundred species and a few thousand elementary reactions together with multi-species thermodynam-

August 28 - 30, 2013 Poitiers, France

ics and transport, this is not possible when one considers turbulent flames. In most practical applications, the flow is turbulent because it enhances mixing and promotes chemical conversion. The description of turbulent combustion thus constitutes a central problem which requires a clever and well balanced handling of the complexities of the process. Prediction of the approximate length of a flame in a glass furnace does not need a detailed consideration of the chemical kinetics and a simplified one-step chemistry may well be sufficient to predict the burning velocity in turbulent premixed flames (Roux *et al.*, 2005). But this extreme simplification of chemical kinetics is no longer adequate when one wishes to consider phenomena which are sensitive to the chemical mechanisms such as the formation of pollutants like carbon monoxide, nitrogen oxides, unburned hydrocarbons or soot or when one wishes to analyze the ignition delay. These questions cannot be answered without taking into account some of the chemical kinetics complexity. Chemical composition and elementary reactions also influence flame stabilization in continuous combustion systems like gas turbines which are partially premixed and they control ignition, flame propagation and interactions with walls in internal combustion engines. In IC engines, fuel and air are diluted by exhaust gas recirculation (EGR) and the flame becomes sensitive to low concentrations of radical species produced during the initiation phase of combustion. The challenges are even greater in the case of pollutant predictions because of their considerably smaller concentrations and the many pathways leading to their formation or destruction. Pollutant mole fractions amount to a few tenths to a few hundreds ppms while the main species are in much larger proportions (a few percentage points and about 70% for nitrogen which acts as a diluent). This large dynamic range constitutes a real challenge for predictions.

While there are uncertainties in reaction kinetics many detailed chemical mechanisms have been developed in recent years with an increasing degree of complexity to account for the chemical conversion of heavier hydrocarbons. Current schemes in combination with detailed models provide good predictions of laminar burning velocities of flames formed by light hydrocarbons like methane (Smith *et al.*, 1999). Heavier hydrocarbons like n-decane, the main constituent of kerosene can also be considered with a reasonable degree of accuracy (Dagaut & Cathonnet, 2006). The determination of some polluting species, like soot, is not as firmly established but a basis is available which can be included in simulation models and may be used to guide analysis and design.

Introduction of detailed chemical kinetics in numerical simulations, raises difficult modeling issues and practical problems of computational strategy and resources. Since each species in the reaction scheme requires the solution of a transport equation, it is clearly not possible to think that this can be handled in multidimensional simulations within a finite CPU time except for some simple flames. The problem is compounded in the case of turbulent flames where it is usually difficult to handle detailed reaction schemes except again in some special cases. Direct numerical simulations (DNS) have been carried out for hydro-

gen or light hydrocarbon combustion but with important limitations on the the computational domain size, which does not in general exceed a few cm in the three directions. Simulations based on Reynolds-Averaged Navier-Stokes (RANS) and Large Eddy Simulations (LES) require the establishment of closure laws for the rates of reaction and a strategy to reduce the complex kinetics to a computationally tractable description. These two aspects are considered in what follows.

This article begins with a brief review of turbulent combustion modeling. Chemistry modeling routes are examined in a second step. The central problem of coupling of chemistry with a large eddy simulation is considered in a third step. Examples of turbulent combustion simulations are discussed in the final part of this article.

## SYNTHETIC REVIEW OF TURBULENT COMBUSTION MODELING

One essential difficulty in turbulent combustion is the multiplicity of spatial and temporal scales. The competition of turbulent mixing and chemical reaction gives rise to a variety of turbulent flame structures (see for example Veynante & Vervisch (2002); Poinot & Veynante (2005)). The modeling of the rate of heat release in turbulent streams constitutes a central issue which has been extensively investigated. Initial efforts were focused on devising models for Reynolds Average Navier-Stokes equations (RANS). More recent research has addressed issues of direct simulation of turbulent flames and Large Eddy Simulations (LES). It is useful to review these three levels of simulation and provide a historical perspective.

### Reynolds averaged Navier-Stokes equations

RANS methods have provided useful estimates of mean quantities but their predictive capacity are known to be limited. One difficulty in this framework is to derive a representation of the mean reaction rates, a problem which may be handled in many different ways. Early models were founded on the idea that the rate of conversion and heat release were controlled by mixing. This has resulted in the eddy-break up or eddy dissipation models where the mixing characteristic time was deduced from the turbulence closure. Another representation of the mean reaction rate has relied on probability density functions (PDF). The mean value of the reaction rate is determined by summing the instantaneous rate over probability space. In the simplest case of a single step reaction it is possible to describe species and temperature in terms of a unique progress variable  $c$ . A one variable PDF is only needed in this case  $p(c)$  (see for example Borghi (1988)) and the mean reaction rate may be cast in the form :

$$\bar{\omega} = \int \dot{\omega}(c)p(c)dc \quad (1)$$

The PDF is most often presumed and its free parameters are adjusted by making use of moments of the progress variable. Another possibility which has been

extensively explored is to solve an evolution equation for the pdf. In a multispecies case this requires additional modeling and considerable computational resources. The mean reaction rate can also be determined by considering the regime of combustion and using additional assumptions. One of them has been to consider that chemical conversion takes place in identifiable flame structures designated as flamelets. This has been explored in much detail and most notably by Peters (see for example Peters (1984, 1986, 2000)). Another method has been founded on the idea that the flame surface density could be quantified with some algebraic or additional transport equations. This possibility is exploited in flame surface density (FSD) models like the Coherent Flame Model introduced by Marble and Broadwell Marble & Broadwell (1977). CFM and its extensions rely on a balance equation for the mean flame surface density  $\Sigma$  (Darabiha *et al.* (1989); Candel & Poinso (1990); Candel *et al.* (1990)). A balance equation for  $\Sigma$  is derived from first principles and used to represent unsteady accumulation, convection, diffusion, production and destruction of flame surface area in the turbulent flow. The mean reaction rate is obtained by weighting the flame surface density by the local reaction rate per unit flame surface. This latter quantity can be obtained from a local flame structure analysis relying on multi-species kinetics and transport calculations. The local flame sheet is most often represented as a strained flame. It is used to account for strain rate effects on the reaction rate. In non-premixed flames this is quite important because the reaction rate per unit surface increases like the square root of the strain rate  $\dot{m} \approx \epsilon_s^{1/2}$  if the strain rates are sufficiently low compared to the critical extinction value. FSD models have been successfully used in the field of internal combustion engines, most notably by Boudier *et al.* (1992); Baritaud *et al.* (1996); Helie & Trouv  (2000); Colin *et al.* (2003); Colin & Truffin (2010).

### Direct numerical simulations

While the initial RANS developments were based on theory, dimensional analysis and comparisons with experimental data, direct numerical simulation (DNS) introduced at a later stage (around the end of the 1980s) have provided considerable insight on the combustion process serving as a guide for modeling. DNS became feasible as a result of progress in higher order numerical methods, derivation of characteristic boundary conditions for the Navier-Stokes equations (NSCBC) by Poinso & Lele (1992) and augmented computational resources. At the turn of the 1980s it became possible to examine interactions between flames and turbulence. The initial calculations were carried out by considering a square or cubic domain of turbulence and examining a flame in this configuration (Poinso *et al.* (1996); Poinso (1996); Vervisch & Poinso (1998)). Many simulations were initially carried out in two dimensions while three dimensional direct simulations were reported after a short delay by Trouv  *et al.* (1994); Th venin *et al.* (2002); Th venin (2005). DNS has allowed exploration of ignition and autoignition, turbulent flame structures, lifted flames, flame interactions with boundaries.

Some recent simulations of turbulent flame struc-

tures and burning velocities carried out by Poludnenko & Oran (2010, 2011) provide considerable insight on the process of flame propagation in turbulence. Most calculations were carried on regular grids with a constant mesh size allowing to simultaneously resolve all turbulence scales (from the integral scale  $l$  to the dissipative scale  $l_k$ ) and all flame scales. With the availability of high performance computational resources, direct simulations addressed more complex situations like lifted jet flames (Mizobuchi *et al.* (2002)), laboratory scale turbulent "V"-flame (Bell *et al.* (2005)) and swirling flows Moureau *et al.* (2011a,c).

### Large eddy simulations in combustion

While Reynolds average methods are limited to the analysis of the mean flow field and cannot be expected to yield a high fidelity description of the turbulent flow, direct simulations retrieve the details of the flow and its interaction with the flame but are limited to low Reynolds number flows and are restricted to relatively small computational domains. In this context, large eddy simulations (LES) constitute an interesting strategy for numerical simulations of turbulent combustion. In LES the large scale energy containing eddies are calculated while subgrid models are used to represent the smaller scales. Since most reacting flows exhibit large scale structures, especially when thermo-acoustic instabilities occur, this description is specifically attractive and it may be expected to be particularly effective combustion dynamics analysis. LES provides an improved framework for the description of turbulence/combustion interactions because large structures are calculated explicitly. The simulation also clearly identifies instantaneous fresh and burnt gases zones, where turbulence characteristics are notably different. While LES is relatively well established in aerodynamics its applicability to combustion is more recent, with the first applications dating back to the 1990s. Pioneering calculations of this type due to Menon & Jou (1991b) demonstrate applications to ramjet combustion instabilities. Combustion LES raises a number of issues which are addressed in many recent investigations of reacting flows (see Poinso & Veynante (2005) for a broad presentation and Westbrook *et al.* (2005); Pitsch (2006); Pitsch *et al.* (2008); Bockhorn *et al.* (2009) for recent reviews). The central questions in combustion LES concern subgrid scale modeling of reaction rates, integration of complex chemistry features, description of pollutant formation and destruction like CO, NOx and soot. There are many other issues and in particular that of spray injection and combustion.

In practice, LES relies on spatial averaging of the balance equations. The spatially filtered variables are formally defined by an expression of the form:

$$\overline{Q(x,t)} = \int Q(x',t)F(x-x')dx' \quad (2)$$

where  $F(x)$  is a filter function. When this filtering operation is applied to the instantaneous balance equations, one obtains spatially filtered expressions including unresolved Reynolds stresses and heat and species fluxes and spatially filtered heat release and reaction

rates. One issue in LES is the definition of a model providing the spatially filtered reaction rates, a problem which has received considerable attention in recent years and which will be discussed later on in this article.

## CHEMISTRY MODELING ROUTES

The full description of chemical reactions in hydrocarbon flames implies hundreds of species and thousands of reactions. There are some major difficulties in handling detailed chemical schemes in turbulent combustion: (i) An additional balance equation is required for each species; (ii) Chemical reaction rates and transport coefficients are complex functions of species mass fractions and temperature. Increasing the number of chemical reactions increases the computational time; (iii) A major theoretical difficulty, often neglected: chemical reactions involve a wide range of spatial and time scales and their coupling with turbulence cannot be summarized to a single time scale. This section briefly presents the main routes to include finite rate kinetics in numerical simulations.

### Detailed chemistry formalism

The thermo-chemical state of a system is described by the vector  $\varphi$ , which includes temperature, species mass fractions, and chemical reaction rates.  $\varphi$  is identified from two state variables and from the chemical composition (Maas & Pope, 1992). If the pressure  $p$  and the temperature  $T$  are retained as state variables, then a function  $\mathcal{F}$  exists such that:

$$\varphi = \mathcal{F}(p, T, Y_1, Y_2, \dots, Y_{n_{sp}}) \quad (3)$$

where  $Y_k$  is the mass fraction of the  $k^{th}$  species and  $n_{sp}$  is the total number of chemical species considered in the chemical mechanism.

The mixture enthalpy  $h$  and internal energy  $e$  are respectively given by:

$$h = h^0 + \int_{T^0}^T c_p dT \quad (4)$$

$$e = e^0 + \int_{T^0}^T c_v dT \quad (5)$$

where  $c_p$  and  $c_v$  are the specific heats of the mixture at constant pressure and volume, respectively. The superscript <sup>0</sup> represents the reference state. Under the perfect gas assumption, the mixture density is related to the pressure, temperature and mixture composition by:

$$\rho = \frac{p}{rT} \quad (6)$$

where  $r = R/W$  with  $R = 8.314 \text{ J}\cdot\text{mol}^{-1}\cdot\text{K}^{-1}$  the perfect gas constant and  $W$  the mixture molar mass. Equations 4, 5 and 6 enable the substitution the pair  $(p, T)$

by  $(p, h)$  or  $(\rho, e)$ . It is then possible to express the thermochemical state in terms of these new set of variables :

$$\varphi = \mathcal{G}(p, h, Y_1, Y_2, \dots, Y_{n_{sp}}) \quad (7)$$

$$\varphi = \mathcal{H}(\rho, e, Y_1, Y_2, \dots, Y_{n_{sp}}) \quad (8)$$

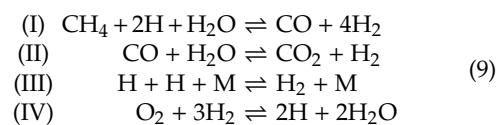
The objectives of detailed chemistry are to reproduce, with the highest possible precision, chemical pathways (or at least the most important pathways) involved in combustion. A detailed scheme is an exhaustive list of all possible elementary reactions between all species involved in the conversion process of a given fuel and oxidizer. Ideally, a reference detailed scheme would be valid for the entire possible range of thermodynamical states (pressure, temperature) and compositions (fuel/air equivalence ratio, fuel and oxidizer dilution, ...). Except for the lighter hydrocarbons, there are no unique detailed kinetic schemes. Moreover, the development of detailed mechanism is also not the final answer to flame chemistry modeling. When the mechanism is too large it cannot be effectively used in multidimensional simulations of flames.

In detailed chemistry simulations, one balance equation must be solved for each chemical species involved in the chemical mechanism. The associated computational cost may become prohibitive for large chemical mechanisms. Even for simple flames the number of transport equations and state variables may become too large to allow easy convergence to the solution. There are however alternative modeling strategies which can be roughly divided in three groups, namely *reduced chemistry*, *global chemistry* and *tabulated chemistry*. The objective is in all cases to reduce the degree of freedom of the thermochemical state. It is convenient to give at this point a brief overview of these three methods.

### Reduced and global chemistry

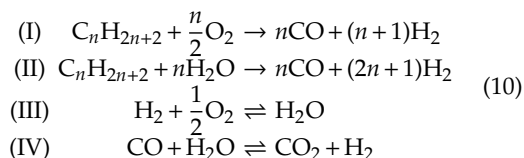
The development of reduced schemes from detailed chemical kinetics can be done "by hand" and relies on two main assumptions: (i) *quasi-steady state approximation*: some (fast) intermediate species or radicals are assumed to have reached an equilibrium state. Their mass fractions are nearly constant and their overall reaction rates negligible; (ii) *partial equilibrium*: some elementary reactions in the chemical scheme are assumed to have reached equilibrium. These assumptions decrease the number of species and reactions involved, leading to mechanisms with a narrower range of validity.

For example, starting from a detailed mechanism, Peters (1985) proposes a four-step global chemical scheme for methane, including seven species (see also Peters, 2000):



where the four reaction rates are determined from limiting steps of the chemistry, under quasi-steady state

and partial equilibrium approximations (Peters, 1985). A similar analysis was carried out by Jones & Lindstedt (1988) for hydrocarbons  $C_nH_{2n+2}$  up to butane ( $n = 4$ ) leading to the four-step global chemical scheme:



The corresponding rate constants are given in Jones & Lindstedt (1988). Reduced schemes raise many issues. For example one notes that the global reaction rate of the third reaction involves a negative water concentration exponent, which may lead to practical difficulties in numerical simulations. The authors propose an alternative formulation avoiding such a dependence but providing a reduced accuracy in fuel lean regions.

The design of short mechanisms, useful for multi-dimensional simulations, is even more difficult when one considers heavy hydrocarbons fuels. Automatic reduction methods have been proposed to reduce complex mechanisms but only to a skeletal level, where hundreds of species are still retained. A pragmatic alternative has been proposed by Franzelli *et al.* (2010) to extract a two-step scheme for kerosene-air flame. To fit the laminar burning velocity over a wide range of operating conditions, the pre-exponential constants of the two reactions are tabulated as a function of the local equivalence ratio. The fuel and oxidizer exponents are chosen to guarantee the correct dependence of premixed laminar burning velocity with mean pressure.

The formulation of global chemical schemes is attractive but leads to various difficulties. First, the identification of limiting steps, quasi-steady state species and equilibrated reactions in a detailed chemical scheme requires an expertise in chemical kinetics. In addition, the reduction in terms of computational costs is lower than expected: the number of species and reactions is decreased but reaction rates have more complicated expressions and the system of algebraic equations combined with the standard reaction rate terms becomes mathematically stiffer. These reaction rates can also feature molar concentrations with negative exponents leading to practical difficulties, especially in the initiation of the simulation.

## Tabulated chemistry

**Principle.** Tabulated chemistry aims at expressing the thermochemical variables in a reduced chemical state space, compared to detailed chemistry formalism. The set of species mass fractions involved in Eqs. 3, 7 or 8 are replaced by a reduced set of coordinates  $(\psi_1, \psi_2, \dots, \psi_n)$ , where  $n+2$  is the number of dimensions of the thermochemical database. Tabulated chemistry is efficient in comparison with detailed chemistry if  $n \ll n_{sp}$ . In this new basis, example of the thermochemical variables  $\varphi$  expressions are:

$$\varphi = \mathcal{F}'(p, T, \psi_1, \psi_2, \dots, \psi_n) \quad (11)$$

$$\varphi = \mathcal{G}'(p, h, \psi_1, \psi_2, \dots, \psi_n) \quad (12)$$

$$\varphi = \mathcal{H}'(\rho, e, \psi_1, \psi_2, \dots, \psi_n) \quad (13)$$

In practice, the mathematical functions  $\mathcal{F}'$ ,  $\mathcal{G}'$  or  $\mathcal{H}'$  do not have analytical expressions. They are usually defined in the discrete form of a database explaining the designation *tabulated chemistry*. As the chemical database construction involves a chemical mechanism, tabulated chemistry is always a degraded representation of detailed (or skeletal) chemistry.

The key issues in the tabulated chemistry framework are to identify a suitable set of coordinates  $(\psi_1, \psi_2, \dots, \psi_n)$  and to generate the appropriate chemical database. The numerous strategies proposed for that purpose can be classified in two groups which rely on mathematical and physical analysis, respectively.

A pioneering mathematical technique for chemistry tabulation is the ILDM (Intrinsic Low-Dimensional manifold) method, devised by Maas & Pope (1992). This is based on a direct identification of the dynamic behavior of the nonlinear response of the chemical system. An attractor subspace is determined by examining the eigenvalues and eigenvectors of the system of equations and by neglecting and cutting-off fast time-scales smaller than a given time limit. Depending on the cut-off time-scale, one, two or more coordinates of this state space (equivalent to chemistry parameters) are enough to accurately reproduce the kinetic properties of the full reactive system. This attractor subspace is called manifold and the number of its coordinates corresponds to the minimum number of scalars that need to be transported to describe the full reactive system. In general, highly-reduced ILDM manifolds (maximum two coordinates) do not correctly reproduce the low-temperature regions of the flame, sensitive to molecular diffusion (Gicquel *et al.*, 1999).

An alternative is to include physical consideration for designing the chemical database. This assumption is the foundation of flamelet models which assume that a turbulent flame front can be decomposed in a collection of 1-D flame elements. This strategy, originally developed by Peters (1984) and Bradley *et al.* (1988) for turbulent non-premixed and premixed flames respectively, is effective and well adapted to complex geometry reactors. Details and examples of flamelet based tabulated chemistry techniques are given in the following sections. The principal coordinates of tabulated chemistry are first introduced.

**Principal coordinates of tabulated chemistry** The role of the chemical look-up table coordinates is to capture the impact of kinetics, molecular diffusion and heat losses on the flame structure. As the number and definition of the control variables depends on the modeling assumptions, there is no universal set of coordinates. Issues encountered in trying to represent the influence of dominant phenomena on combustion chemistry are discussed in what follows.

*Capturing mixing phenomena*

Mixing between fuel and oxidizer streams is usually described by a conserved scalar, the mixture fraction  $Z$ . There are many possible definitions which depend on chemistry and transport modeling assumptions (Poinsot & Veynante, 2005).

The simplest formulation of the mixture fraction can be derived for a single step chemistry of the type:  $\nu'_F F + \nu'_O O \rightarrow P$  where  $F$ ,  $O$  et  $P$  are fuel, oxidizer, and products, respectively and  $\nu'_F$  and  $\nu'_O$  denote molar stoichiometric coefficients. Assuming that molecular diffusivity are identical for all species, a possible definition of the mixture fraction is :

$$Z = \frac{sY_F - Y_O + Y_O^o}{sY_F^f + Y_O^o} \quad (14)$$

where superscripts  $o$  and  $f$  refer to the fuel and oxidizer stream properties, respectively and  $s = \nu'_O W_O / \nu'_F W_F$  is the mass stoichiometric coefficient. The mixture fraction  $Z$  is equal to 0 and 1 in the fuel and oxidizer streams, respectively.

This definition is not adapted anymore if multi-step chemical schemes are considered. Indeed, because of the presence of intermediate species, Eq. 14 does not ensure that  $Z$  is a conserved scalar. A solution is to base the mixture fraction definition on the element (atomic) mass fractions  $Y_e$  (Masri *et al.*, 1988). For each element  $e$ , a mixture fraction  $Z_e$  is defined as follow:

$$Z_e = \frac{Y_e - Y_e^o}{Y_e^f - Y_e^o} \quad (15)$$

where  $Y_{e_f}$  and  $Y_{e_o}$  are the mass fractions of element  $e$  in the fuel and oxidizer streams, respectively. Even in detailed chemistry situation,  $Z_e$  always remains a conserved scalar. When assuming that all species have constant mass diffusivity ( $Le = \lambda / (\rho c_p D) = 1$ ), the mixture fraction definition does not depend on the chosen element  $e$  ( $Z = Z_1 = Z_2, \dots = Z_l$ , where  $l$  is the total number of elements). Mixing between fuel and oxidizer is then captured by a unique dimension and  $Z = Z_e$  is a conserved scalar described by a balance equation with no chemical source term:

$$\frac{\partial \rho Z}{\partial t} + \frac{\partial \rho u_i Z}{\partial x_i} = \frac{\partial}{\partial x_i} \left( \rho D \frac{\partial Z}{\partial x_i} \right) \quad (16)$$

where the molecular diffusion velocity is modeled by the Fick law. When differential diffusion of species is considered ( $Le_k \neq 1$ ), mixing between fuel and oxidizer is not captured by a unique variable  $Z_e$ . Definition of  $Z$  by Eq. 15 depends on the element considered ( $Z \neq Z_1 \neq Z_2, \dots \neq Z_l$ ). The degree of freedom of the systems increases from 1 to  $l-1$ . Tracking all mixing states then requires to solve a balance equations for each conserved scalar  $Z_e$ , which exhibits unclosed cross-derivative terms. Solutions have been recently proposed by Regele *et al.* (2013) or Maragkos *et al.* (2013) to capture differential diffusion within tabulated chemistry formulations. However, the computational cost and complexity of the look-up table generation are

augmented. A solution is to allow the incorporation of differential diffusion effects by limiting fuel/oxidizer mixing to a single dimension. A unique mixture fraction is used which is generally defined as a conserved scalar solution of Eq. (16) (Pitsch & Peters, 1998, see). While this introduces errors as pointed out by Sutherland *et al.* (2005) it also allows to incorporate differential diffusion features in turbulent flame simulations (Mercier *et al.*, 2013) without affecting the computational cost.

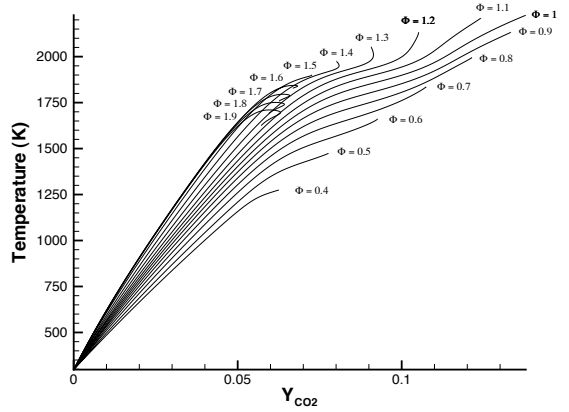
Many practical combustion applications cannot be treated as a two-streams mixing problem between fuel and oxidizer with fixed composition in each stream. This is the case for instance in MILD combustion (Cavaliere & de Joannon, 2004), where reactions are strongly influenced by the rate of fresh gas dilution by burnt products. At least one supplementary coordinate is therefore needed to represent the chemical flame structure and the pollutant formation (Ihme & See, 2011; Lamouroux *et al.*, 2013). A similar problem is observed when fuels with different compositions are injected into a combustion chamber. Two mixture fractions have been introduced for that purpose to capture a three-stream mixing problem (Hasse & Peters, 2005; Naudin *et al.*, 2006).

#### Tracking chemical reactions

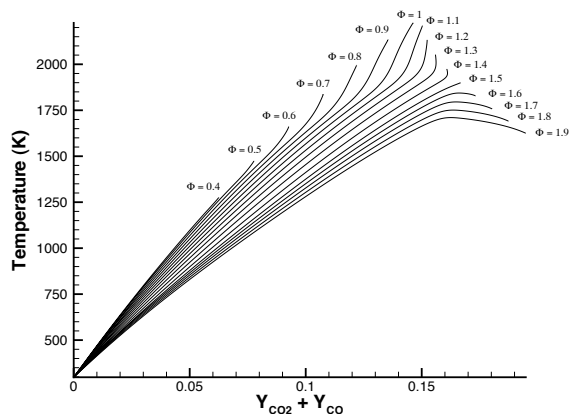
The conversion from fresh to burnt gases is usually captured by the progress variable  $Y_c$  which is generally defined by a combination of species mass fraction, selected to ensure a continuous and monotonic evolution of the progress variable between initial ( $Y_c = Y_c^f$ ) and final ( $Y_c = Y_c^b$ ) states. If this condition is satisfied, then  $\varphi(Y_c)$  is a mapping of  $Y_c$  and the thermochemical variables can be tabulated in term of  $Y_c$ .

The importance of the definition of this progress variable  $Y_c$  is illustrated in Fig 1(a) which shows the projection of methane/air freely propagating adiabatic laminar flames onto the  $(Y_{CO_2}, T)$  space for different values of fresh gas equivalence ratio. From  $\phi = 0.4$  to  $\phi = 1.2$  the temperature expressed as a function of  $CO_2$  mass fraction is bijective, but this ceases to be the case in rich regions where turning points exist. This phenomenon corresponds to the presence of  $CO_2$  and  $CO$  under rich conditions and at high temperature levels. At the same time, for equivalence ratios greater than 1.5, the temperature decreases when  $Y_{CO_2}$  increases. Indeed, during the last chemical steps, where species react and progress towards the equilibrium state, endothermic reactions become more important than the exothermic ones and heat is absorbed instead of being released. A progress variable based on a linear combination of  $CO_2$  and  $CO$  mass fractions as a progress variable,  $Y_c = Y_{CO_2} + Y_{CO}$ , will reduce the importance of the turning point problem. Here the definition of the progress variable is based on a "user" knowledge but may not be optimal. Indeed minor species may still evolve in a non-monotonic fashion and this may introduce some problems in the database exploitation. The progress variable definition may be facilitated by an automatic process which was recently devised by Ihme *et al.* (2012) and Niu *et al.* (2013).

The definition  $Y_c = Y_{CO_2} + Y_{CO}$  is well adapted to the tracking of reactive and thermal layers, but alternative definitions of  $Y_c$  are needed to capture phenomena



(a)  $Y_c = Y_{CO_2}$



(b)  $Y_c = Y_{CO_2} + Y_{CO}$

Figure 1. Projection of 1-D premixed laminar flame trajectories in the plane  $(Y_c, T)$  for two progress variable definitions. Each trajectory corresponds to a given value of fresh gases equivalence ratio  $\phi$  (Fiorina *et al.*, 2003).

that are out of the range of time scales associated to the formation of carbon monoxide and dioxide. This is the case of auto-ignition which exhibits time scales shorter than those of CO and CO<sub>2</sub> production. To account for the ignition delay one has to add the fuel mass fraction in the progress variable definition (Embouazza, 2005; Galpin *et al.*, 2008a; Vicquelin, 2010; Tudorache *et al.*, 2011). Another issue, related to the capture of NO<sub>x</sub> produced through the thermal pathway, is illustrated in Fig. 2. Chemical trajectories followed by a collection of 1-D premixed flames are plotted in the  $(Y_c, Y_{NO_x})$  chemical subspace. For a definition of  $Y_c$  based on CO and CO<sub>2</sub> species important variations of NO<sub>x</sub> are not captured by the progress variable. The first solution, proposed by van Oijen & de Goey (2009) and Godel *et al.* (2009) is to include a selection of nitrogen containing species in the definition of  $Y_c$ . NO trajectories are then mapped by  $Y_c$ , as shown in Fig. 2.

An alternative, which does not constrain the major product to the NO<sub>x</sub> formation, is to introduce two progress variable of which one is dedicated to tracking

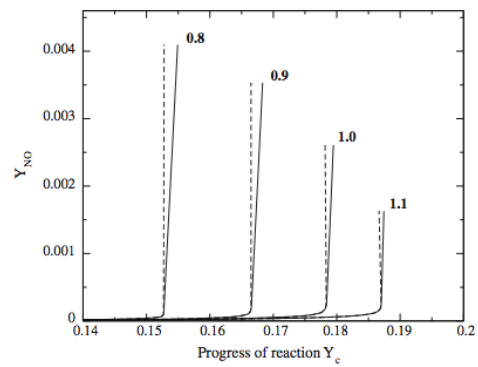


Figure 2. Projection in the space  $(Y_{NO}, Y_c)$  of 1-D premixed laminar flame trajectories obtained for different fresh gases equivalence ratio. Dashed:  $Y_c$  is defined by  $Y_c = Y_{CO} + Y_{CO_2}$ . Solid :  $Y_c$  is defined by  $Y_c = Y_{CO_2} + Y_{CO} + Y_{H_2O} + Y_{NO} + Y_{NO_2} + Y_{N_2O} + \Delta Y_{N_2}$  (Godel *et al.*, 2009).

the flame thermal layer while the other is used to describe nitrogen oxides (Ihme & Pitsch, 2008; Pecquery *et al.*, 2013).

#### Accounting for heat exchanges

It is convenient to use the total (sensible plus chemical) enthalpy  $h = \int_{T_0}^T c_p dT + h^0$  to track effects of heat exchange. Indeed the tabulation procedure remains simple as the sensible plus chemical enthalpy  $h$  is conserved across constant pressure flames, for a given elemental composition.<sup>1</sup> The introduction of a normalized form of the enthalpy, independent of the mixture fraction is convenient in two-stream mixing problems:

$$h_n = \frac{h - h_{min}(Z)}{h_{ad}(Z) - h_{min}(Z)} \quad (17)$$

where  $h_{ad}$  and  $h_{min}$  are the adiabatic and an arbitrary minimal mixture enthalpy, respectively.

**Tabulation strategies** An exhaustive review of strategies devised to build chemical look-up tables would be too long for the present article. One would have to include methods based on time scale analysis, mainly derived from CSP (Lam & Goussis, 1988) and ILDM (Maas & Pope, 1992) theories but this would require additional space. It was decided to focus on flamelet-based tabulation techniques, which are well adapted to the simulation of many types of isobaric or nearly isobaric combustors. Again for the sake of compactness tabulated chemistry methods specifically designed for internal combustion engines, such as the Tabulated Kinetic of Ignition (TKI) model (Colin *et al.*, 2005; Jay & Colin, 2011), will not be discussed in what follows.

#### Premixed flamelet tabulation

<sup>1</sup> $h$  is conserved for isobaric closed systems whereas the sensible plus chemical internal energy remains constant in constant volume reactors.

Premixed flamelet tabulation has been first introduced in RANS computations of turbulent premixed and partially-premixed flames by Bradley *et al.* (1988, 1998). By analyzing DNS results, Gicquel *et al.* (2000) observed that the manifold covered by turbulent premixed flames are well approximated by the trajectory followed by a 1-D laminar flame element. By assuming that diffusion fluxes across mixture fraction iso-surfaces do not alter the chemical flame structure, the properties observed by Gicquel *et al.* (2000) justify the mapping of the chemical trajectories accessed by a partially-premixed (or stratified) flame by a collection of premixed flamelets. A thermochemical look-up table is then formed by solving, in a detailed chemistry framework, the governing equations of a planar laminar premixed flame. The inlet boundary conditions of the calculated flamelets are written in terms of the fresh gas mixture fraction  $Z$ :

$$T^u = T^u(Z), \quad Y_k^u = Y_k^u(Z) \quad \text{for } Z_l < Z < Z_r \quad (18)$$

where  $^u$  superscript refers to fresh gas conditions and  $Z_l$  and  $Z_r$  are the lean and rich flammability limits, respectively. The computation of the premixed flamelet balance equation can be achieved with a dedicated solver, as PREMIX developed by Kee *et al.* (1985), with the boundary conditions prescribed by Eq. 18. Solutions are the thermochemical variables  $\varphi$ , expressed in term of  $x$ , the spatial coordinate normal to the flame front, and the mixture fraction  $Z$ .

$$\varphi = \varphi(Z, x) \quad (19)$$

By definition, the progress variable  $Y_c$  follows a monotonic and continuous evolution between fresh and burnt gas states in the spatial direction  $x$ . The following mapping of any thermo-chemical variable  $\varphi$  is therefore possible:

$$\varphi = \varphi(Y_c, Z) \quad \text{for } Z_l < Z < Z_r \quad (20)$$

Outside the flammability range, chemical reactions rates are equal to zero. Thermochemical variables and mixture composition are estimated by a linear interpolation in  $Z$  space:

$$\text{if } Z_r < Z < 1: \quad \varphi(c, Z) = \frac{Z - Z_r}{1 - Z_r} (\varphi_{fuel} - \varphi(c, Z_r)) + \varphi(c, Z_r) \quad (21)$$

$$\text{if } 0 < Z < Z_l: \quad \varphi(c, Z) = \frac{Z}{Z_l} (\varphi(c, Z_l) - \varphi_{oxy}) \varphi_{oxy} \quad (22)$$

$\varphi_{fuel}$  and  $\varphi_{oxy}$  characterize the fuel and oxidizer thermochemical state, respectively.

This tabulation procedure assumes that combustion occurs under adiabatic conditions. Accounting for effects of heat exchanges on the chemical flame structure requires to include in the look-up table flamelet

solutions obtained under different enthalpy conditions. One possibility is to calculate a series of burner-stabilized flames (van Oijen *et al.*, 2001; Fiorina *et al.*, 2003). Heat losses from each flamelet are controlled by the fresh gas mass flow rate injected through the porous burner. The enthalpy coordinate is then added to the chemical look-up table and each thermochemical variable  $\varphi$  can be expressed in the form:

$$\varphi = \varphi^{FPI}(h, Y_c, Z) \quad (23)$$

Chemistry tabulation based on premixed flamelets are found in the literature under the acronyms FPI (Flame Prolongation of ILDM) or FGM (Flamelet Generated Manifold). This strategy implicitly assumes that a turbulent stratified flame front can be decomposed in a series of independent premixed flamelets. This is true for low fuel/air mixing rates but is questionable when diffusion across mixture fraction iso-layers becomes important (Fiorina *et al.*, 2005). When this happens the structure of the flame sheet is closer to that of a non-premixed flamelet. Chemistry tabulation based on 1-D diffusion flamelets, discussed below, is then more suitable.

#### Non-premixed flamelet tabulation

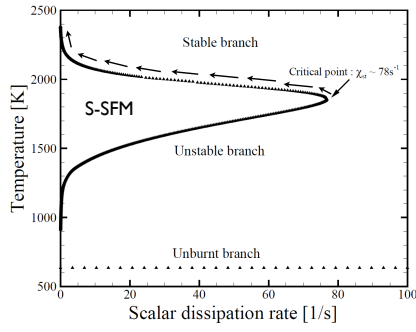
To model non-premixed combustion, Peters (1984) compiled strained steady diffusion flamelets in a thermochemical library. The flamelet equations are generally expressed and solved in the mixture fraction space, where the impact of strain rate on the flame structure is governed by the scalar dissipation rate of the mixture fraction  $\chi_z = D_z |\nabla Z|^2$ . For instance, under unity Lewis number assumption, the species mass fraction are governed by:

$$\rho \frac{\partial Y_k}{\partial t} = \chi_z \frac{\partial^2 Y_k}{\partial Z^2} + W_k \dot{\omega}_k \quad (24)$$

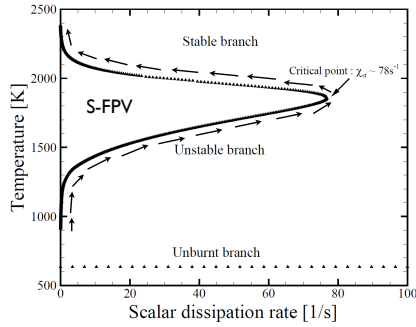
where  $\dot{\omega}_k$  and  $W_k$  are the chemical molar reaction rate and molar mass of the  $k^{th}$  species, respectively. The steady-state solutions of Eq. 24 lead to the identification of thermo-chemical variables  $\varphi$ :

$$\varphi = \varphi^{S-SFM}(Z, \chi_{z_{st}}) \quad \text{with } 0 < \chi_{z_{st}} < \chi_{z_{st}}^q \quad (25)$$

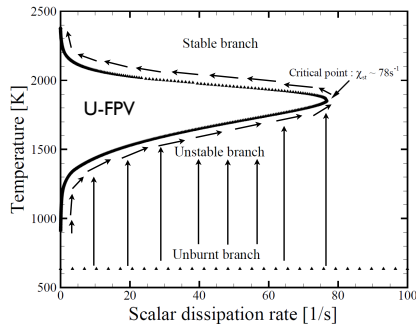
where S-SFM refers to Steady Strained Flamelet Model. In the previous expressions  $\chi_{z_{st}}$  is the mixture fraction scalar dissipation rate conditioned by stoichiometric conditions. This formulation tracks steady states of non-premixed flames, from chemical equilibrium ( $\chi_{z_{st}} = 0$ ) to quenching ( $\chi_{z_{st}} = \chi_{z_{st}}^q$ ). To account for re-ignition events, Pierce & Moin (2004) added the unstable solutions of flamelet equations in the look-up table. The parametrization given by Eq. 25 ceases to be suitable. Indeed, the S-curve plotted in Fig. 3 indicates that a given value of the scalar dissipation rate  $\chi$  may correspond to stable, unstable and unburned states, a unique thermochemical state is not ensured. This issue is overcome by making use of the progress variable  $Y_c$  instead of  $\chi$ :



(a) Steady Strained Flamelet Model (S-SFM)



(b) Steady Flamelet Progress Variable (S-FPV)



(c) Unsteady Flamelet Progress Variable (U-FPV)

Figure 3. S-curve characteristic of a methane/air flame. The fuel temperature is 298K while the air stream has been preheated to 673K. Trajectories covered in the  $(T_{st}, \chi_{st})$  subspace by S-SFM, S-FPV and U-FPV chemical look-up table are shown by arrows. Projections of the manifold mapped by S-SFM and S-FPV are 1-D but 2-D for the U-FPV model.

$$\varphi = \varphi^{S-FPV}(Y_c, Z) \quad (26)$$

where S-FPV stands for Steady-Flamelet Progress Variable. As the chemical trajectories are restricted to the steady state S-shaped response curve, phenomena which are unsteady such as auto-ignition events can not be captured by FPV look-up tables. To describe the transient evolution of all thermochemical variables during the flame ignition process, the solution of unsteady flamelet balance equations needs to be included (Ihme & See, 2010; Michel *et al.*, 2008).  $\varphi$  variables are

then parameterized in the form of:

$$\varphi = \varphi^{U-FPV}(Y_c, Z, \chi_{Zst}) \quad (27)$$

where "U-FPV" refers to Unsteady-Flamelet Progress Variable approaches. Compared to the steady state flamelet library which is parametrized by two variables, a third coordinate has been added to account for unsteady phenomena. Trajectories covered in the  $(T_{st}, \chi_{st})$  subspace by S-SFM, S-FPV and U-FPV chemical look-up tables are shown in Fig.3. The S-SFM model covers the upper stable branch of the S-curve whereas S-FPV includes the lower unstable branch as well. As a dimension has been added to the chemical database, the U-FPV approach relies on two coordinates in the subspace  $(T_{st}, \chi_{st})$ .

An extension of the FPV model has been recently proposed by Lamouroux *et al.* (2013), to account for the influence of burnt gas dilution. This formulation is specifically attractive in modeling of pollutant formation in flameless or MILD (Moderate or intense low oxygen dilution) combustors. In a non-adiabatic context, thermo-chemical variables then read as follows:

$$\varphi = \varphi^{D-FPV}(Y_c, Z, \alpha, h_{n1}) \quad (28)$$

where "D-FPV" refers to Diluted FPV model.  $\alpha$  is the rate of fresh gas dilution by burnt gases. Note that the influence of heat losses are accounted for by the variable  $h_{n1}$  defined in Eq. 17.

FPV tabulated chemistry methods are obviously well adapted to model the chemical structure of diffusion flames but will fail to recover premixed flame properties, such as laminar flame speed (Fiorina *et al.*, 2005). To model complex flame elements which exhibit both premixed and non-premixed flame structures, multi-regime flamelet tabulation are required.

#### Multi-regime flamelet tabulation

To track multiple flamelet regime within a single look-up table, Bykov & Maas (2007, 2009) and Nguyen *et al.* (2010) proposed to solve the projection of the full set of mass conservation species balance equations into a restricted subset of the composition space. The tangential strain rate of scalar isosurfaces is expressed in the form of the scalar dissipation rates of the control parameters which are for partially premixed combustion:  $\chi_Z = D|\nabla Z|^2$ ,  $\chi_{Y_c} = D|\nabla Y_c|^2$  and  $\chi_{Y_c, Z} = D\nabla Y_c \cdot \nabla Z$ . Analytical models for  $\chi_Z$ ,  $\chi_{Y_c}$  and  $\chi_{Y_c, Z}$  can then be used to integrate o multi-regime flamelet equations expressed in the  $(Y_c, Z)$  subspace. Thermo-chemical variables are then expressed as follows:

$$\varphi^{MF}(Y_c, Z, \chi_Z, \chi_{Y_c}, \chi_{Y_c, Z}) \quad (29)$$

The addition of the scalar dissipation rates as control parameters increases the number of look-up table coordinates enabling the modeling of complex flame structures. An alternative, proposed by Franzelli *et al.* (2013a) is to solve multi-regime flamelet equations in physical space. Premixed, partially-premixed and

non-premixed flame solutions are then merged and mapped in a multi-dimensional chemical look-up table. A priori tests on 1-D counterflow flame configuration show that multi-regime chemical look-up table are required to accurately describe pollutant formation such as carbon monoxides (Franzelli *et al.*, 2013a) and other species which are sensitive to the chemistry details of the chemistry.

### Tabulated chemistry and CFD *Low Mach number and compressible flow formalisms*

Low Mach number is generally assumed to generate a thermo-chemical look-up table. If the reactive flow governing equations are also expressed for low Mach conditions, then the chemistry tabulated formalism is consistent and its implementation straightforward. All thermo-chemical variables are directly estimated, for each numerical iteration, from linear interpolation within the chemical look-up table. For instance, density and temperature of adiabatic reactive flows are expressed in the form:

$$\rho = \rho^{tab}(\psi_1, \psi_2, \dots, \psi_n) \quad (30)$$

$$T = T^{tab}(\psi_1, \psi_2, \dots, \psi_n) \quad (31)$$

Issues appear in the coupling with compressible Navier - Stokes equations, in particular when compressible effects are not taken into consideration during the database generation. By comparison with an adiabatic and isobaric low Mach number flow, the compressible formalism introduces two degrees of freedom which are for instance the pair  $(e, p)$  or  $(e, \rho)$ . Even if the flow is adiabatic, the internal energy will vary locally because of acoustic pressure waves.

To couple an adiabatic chemical table with a compressible flow solver, Galpin *et al.* (2008b) proposed to solve, in addition to the reduced set of variables, balance equations for some chemical species selected to estimate the temperature from energy. This implementation does not require heavy modifications of the flow solver but leads to a large increase in the number of equations. In addition, a divergence between the additional transported species and the tabulated ones is frequently observed and requires a specific treatment.

An alternative, called TTC (Tabulated Thermochemistry for Compressible flows) has been proposed by Vicquelin *et al.* (2011). The first order truncated Taylor expansion of  $e$  around  $T = T^{tab}$  leads to the following linear approximation of the temperature:

$$T = T^{tab}(\psi_1, \dots, \psi_n) + \frac{e - e^{tab}(\psi_1, \dots, \psi_n)}{C_v^{tab}(\psi_1, \dots, \psi_n)} \quad (32)$$

The "compressible" temperature  $T$  can therefore be approximated from the energy and temperature  $e^{tab}$  and  $T^{tab}$  which are both tabulated in an adiabatic look-up table. The energy  $e$  which accounts for acoustic perturbations is transported. Note that this assumption is valid in the case of moderate acoustic perturbations which induce small temperature variations. It is justified when combustion operates at constant pressure

such as in gas turbines, furnaces, unconfined laboratory flames, etc... Other practical situations exist where pressure variations are sufficiently large to affect the chemistry (internal combustion engines, detonation waves, . . .) and extra-coordinates have to be added to the chemical database.

Finally the introduction of tabulated chemistry in compressible CFD requires a careful treatment of boundary conditions. For that purpose, Vicquelin *et al.* (2011) proposed a reformulation of the Navier Stokes Characteristic Boundary Conditions (NSCBC) derived by Poinso & Lele (1992).

### *Managing chemical table storage*

In a parallel computational framework, chemical databases are loaded in the local memory of each processor to minimize data exchanges. Then, the chemical database size may become a problem when handling a large number of coordinates. This issue is of crucial importance when running on massively parallel computers having a limited amount of memory per processor. Some strategies has been developed to limit the chemical database sizes. For example, ISAT (In Situ Adaptive Tabulation) proposed by Pope (1997) relies on the in situ generation of look-up tables, which are constructed from the direct solution of time evolution equations for species mass fractions. Only the chemical composition effectively accessed during the computation are calculated and included in the chemical table. An alternative to reduce the database size is to introduce optimal neural networks to approximate chemical tables (Flemming *et al.*, 2005; Ihme *et al.*, 2007). Another simplification in the framework of premixed flamelet tabulation devised by Ribert *et al.* (2006) exploits self-similar properties of laminar premixed flames to reduce the database memory requirements. It is shown that species reaction rates expressed as a function of a progress variable reduce to single curves when using suitable scaling rules. This strategy has been recently extended to turbulent regimes by taking advantage of self-similar properties of mean chemical quantities under a presumed probability density function formalism (Naudin *et al.*, 2006; Veynante *et al.*, 2008). This idea has been successfully applied to the RANS simulation of a turbulent jet flame (Fiorina *et al.*, 2009).

A different strategy recently proposed by Weise *et al.* (2013) relies on a Memory Abstraction Layer (MAL) that handles requested chemical look-up table entries efficiently by splitting the database file into several smaller blocks. The method keeps the total memory usage at a minimum by employing thin allocation methods and compression to minimize filesystem operations. The efficiency of the method has been demonstrated on the simulation of laminar and turbulent non premixed flames (Weise *et al.*, 2013).

## COUPLING CHEMISTRY WITH LES

One of the central issues in combustion LES is to couple the chemistry description to the large eddy simulation flow solver. This section summarizes the different approaches derived to model reaction rates in this framework. These may be classified with respect to the following two points:

**Flame / Turbulence interactions:** primary modeling concepts may be based on flame surface, statistical and mixing formalisms, as described in the following sections.<sup>2</sup>

**Chemistry description:** The simplest description is to assume that chemical time scales are infinitely fast compared to turbulence scales. The flame is then viewed as a collection of laminar flame elements (flamelet assumption), leading to global descriptions (“mixed is burnt” for non-premixed flames or infinitely thin propagating flame surface for premixed flames). More refined approaches involve simple chemical step, reduced global chemical schemes, skeletal schemes, tabulated chemistry, detailed chemical mechanisms as described in the previous section.

Most of the combinations (flame / turbulence interaction, chemical description) are theoretically possible but not necessarily of practical interest. A third dimension for classification is the practical implementation, considering assumptions made in the solver developments (fully compressible or low Mach number framework) of efficient chemistry implementations, for example through the ISAT formalism (Pope, 1997).

Compared to Reynolds Averaged Navier-Stokes (RANS formalism), two specific issues should be considered (i) First, the instantaneous flame front thickness is generally smaller than the typical mesh size, usually directly linked to the filter size. Combustion is mainly a sub-grid scale phenomenon while most of the turbulence energy is contained in large resolved scales. Models should be adapted to overcome this difficulty but, up-to-now, only flame surface formalism derivations explicitly consider this point and, in practice, the resolved flame thickness is mainly controlled by numerics in most models ; (ii) LES models should be able to reproduce laminar flames when sub-grid scale turbulence vanishes. In contrast most of the RANS models are derived in the limit of high Reynolds number turbulence and do not behave correctly when they are applied in the laminar flow limit. One may remember that LES is expected to reduce to DNS in the limit where the filter size is diminished and becomes vanishingly small  $\Delta \rightarrow 0$ . In addition in the computational meshes accessible today, the flame front wrinkling may become fully resolved in some part of the numerical domain (Fiorina *et al.*, 2010).

Conceptually, the Large Eddy Simulation formalism introduces a numerical length scale, the filter size  $\Delta$ , in the turbulent combustion problem. To compare this new practical scale to turbulence and combustion length scales led Pitsch & Duchamp de la Geneste (2002) to revisit premixed combustion regime diagrams (see also Pitsch (2006) for a discussion of this issue).

<sup>2</sup>Note that several concepts may be combined. For example, partial premixing (i.e., heterogenous equivalence ratio fields) are generally incorporated in flame surface concepts through mixture fraction probability density functions. The classification proposed here is based on the primary modeling concept, flame surface for the previous example.

## Geometrical approach

Three main approaches have been developed describing the flame in terms of flame surface and managing the flame thickness issues discussed previously: G-equation, filtered one-dimensional flames and thickened flame model.

**Level set or “G-equation” formalism** In this approach, the flame surface is viewed as an infinitely thin propagating surface (flamelet). The key idea is to track the position of the flame front using a field variable  $G$ . This  $G$ -field, generally identified to a signed distance to the flame front, does not have to follow the gradients of the progress variable  $c$  and can be smoothed out to be resolved on the LES mesh. The G-equation is introduced by Kerstein *et al.* (1988):

$$\frac{\partial G}{\partial t} + \tilde{\mathbf{u}} \cdot \nabla G = S_T |\nabla G| \quad (33)$$

where  $S_T$  is the sub-grid scale turbulent burning velocity that should be modeled. Equation (33) corresponds to a simple kinematic description and its coupling with the density field through heat release requires some care (Piana *et al.*, 1997; Moureau *et al.*, 2009; Knudsen *et al.*, 2010). However, despite some drawbacks, this approach has become one of the most commonly used in large eddy simulations of premixed combustion (Menon & Jou, 1991a; Peters, 2000; Pitsch & Duchamp de la Geneste, 2002; Schmidt & Klein, 2003; Pitsch, 2005; Wang & Bai, 2005; Pitsch, 2006; Dahms *et al.*, 2008; Knudsen & Pitsch, 2008; Schneider *et al.*, 2008; Moureau *et al.*, 2009).

## Filtering laminar flames

### Basic principles

Applying the LES filter  $F$  to the reduced progress variable  $c = Y_c / Y_c^{eq}$  balance equation in premixed combustion ( $c = 0$  within fresh reactants and  $c = 1$  within burnt products,  $Y_c^{eq}$  being the  $Y_c$ -equilibrium value) leads to the following expression:

$$\frac{\partial \overline{\rho c}}{\partial t} + \nabla \cdot (\overline{\rho \mathbf{u} c}) + \nabla \cdot [\overline{\rho} (\overline{\mathbf{u} c} - \overline{\mathbf{u} c})] = \overline{\nabla \cdot (\rho D \nabla c)} + \overline{\dot{\omega}_c} \quad (34)$$

$$= \overline{\rho w |\nabla c|} \quad (35)$$

where  $\overline{Q}$  and  $\tilde{Q} = \overline{\rho Q} / \overline{\rho}$  denote filtered and mass-weighted filtered quantities, respectively. The three LHS terms correspond respectively to unsteady effects, resolved convective fluxes and unresolved transport. The two RHS terms in Eq. (34) respectively denote filtered molecular diffusion and filtered reaction rate. The RHS term in Eq. (35) corresponds to flame front displacement.

As already pointed out, the flame front is generally too thin to be resolved on the LES computational mesh. Nevertheless, the filtered progress variable  $\tilde{c}$  may be resolved using a physical space Gaussian filter with a filter size  $\Delta$  larger than the computational

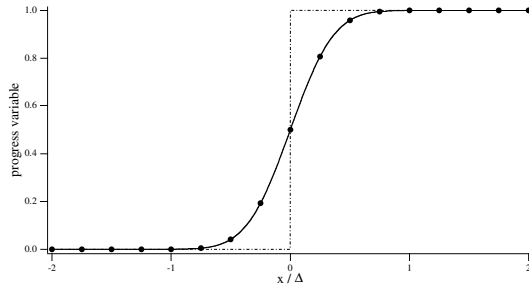


Figure 4. Effect of a spatial Gaussian filter having a size  $\Delta$  larger than the mesh size  $\Delta_m$  ( $\Delta = 4\Delta_m$ ). The unfiltered progress variable  $c$  (dashed-dotted line) and the filtered progress variable  $\bar{c}$  (bold line) are plotted as a function of  $x/\Delta$  where  $x$  is the spatial coordinate. The progress variable  $c$  is not resolved on the computational mesh denoted by ( $\bullet$  symbols) whereas the filtered progress variable  $\bar{c}$  is resolved with about  $2\Delta/\Delta_m = 8$  grid points inside the filtered flame front (Boger *et al.*, 1998).

mesh size  $\Delta_m$  as shown in Fig. 4 (Boger *et al.*, 1998). Accordingly, the filtered flame front is numerically resolved with about  $2\Delta/\Delta_m$  grid points. The  $\bar{c}$ -balance equation (35) is similar to a  $G$ -equation but, compared to an arbitrary  $G$ -field, the progress variable  $c$  has the important advantage of being related to quantities that are physically defined and may be extracted from DNS or experimental data.

Boger *et al.* (1998) then propose a flame surface density formulation for subgrid scale modeling. The flame front displacement may be recast as:

$$\begin{aligned} \overline{\rho w |\nabla c|} &= \int_{-\infty}^{+\infty} \rho w |\nabla c| F(\mathbf{x} - \mathbf{x}') d\mathbf{x}' \quad (36) \\ &= \int_{-\infty}^{+\infty} \int_0^1 \rho w |\nabla c| \delta(c - c^*) F(\mathbf{x} - \mathbf{x}') dc^* d\mathbf{x}' \\ &= \int_0^1 \langle \rho w \rangle_s^* \Sigma^* dc^* = \langle \rho w \rangle_s \Sigma = \langle \rho w \rangle_s \Xi |\nabla \bar{c}| \end{aligned}$$

where  $\delta$  is Dirac's delta function.  $\Sigma^*$  is the sub-grid surface density (i.e. the subgrid surface per unit volume) of the  $c = c^*$  surface and  $\langle Q \rangle_s^*$  denotes the conditional averaging of  $Q$  along this surface  $c=c^*$ .  $\Sigma$  and  $\langle Q \rangle_s$ , introduced in Eq. (37) may be viewed as generalized subgrid flame surface density and surface average, defined by:

$$\Sigma = \int_0^1 \Sigma^* dc^* = |\nabla \bar{c}| \quad (37)$$

$$\langle Q \rangle_s = \frac{1}{\Sigma} \int_0^1 \langle Q \rangle_s^* dc^* = \frac{\overline{Q |\nabla c|}}{\Sigma} \quad (38)$$

while  $\Xi = \Sigma/|\nabla \bar{c}|$  is the flame front wrinkling factor.

The challenge is now to model  $\langle \rho w \rangle_s$  and  $\Xi$  or  $\Sigma$ . The first term is related to the internal flame structure while the two others describe the flame / turbulence interaction. Filtered flame models depend on the methods adopted to describe the previous quantities:

- **The Boger *et al.* (1998) model** relies on the ratio of the surface-averaged mass-weighted displacement

speed to the laminar flame speed  $S_L$  and the fresh gas density  $\rho_u$  as  $\langle \rho w \rangle_s \approx \rho_u S_L$ , while  $|\nabla \bar{c}|$  is estimated by filtering one-dimensional infinitely thin laminar pre-mixed flame, approximating the result by a progress variable parabolic shape, leading to:

$$\Sigma = 4\Xi \sqrt{\frac{6}{\pi}} \frac{\bar{c}(1-\bar{c})}{\Delta} \quad (39)$$

To ensure a correct sub-grid scale turbulent burning velocity  $S_T = \Xi S_L$  and recover  $S_L$  when the flame becomes laminar ( $\Xi \rightarrow 1$ ), Boger & Veynante (2000) proposed an adapted model for the unresolved progress variable transport  $\bar{\rho}(\bar{\mathbf{u}}\bar{c} - \bar{\mathbf{u}}\bar{c})$ .

- **Duwig (2007)** proposed to extract  $\langle \rho w \rangle_s |\nabla \bar{c}|$  by filtering one-dimensional synthetic laminar flames using a Gaussian expression for the reaction rate.

- **F-TACLES model:** Fiorina *et al.* (2010) propose to tabulate the unclosed terms by filtering one-dimensional laminar flames derived from detailed chemical simulations, leading to :

$$\begin{aligned} -\nabla \cdot [\bar{\rho}(\bar{\mathbf{u}}\bar{c} - \bar{\mathbf{u}}\bar{c})] &= \Xi \Omega_c^{FTab}(\bar{c}, \Delta) \quad (40) \\ &+ (\Xi - 1) \nabla \cdot (\alpha_c^{FTab}(\bar{c}, \Delta) \bar{\rho} \bar{D} \nabla \bar{c}) \end{aligned}$$

$$\nabla \cdot (\bar{\rho} \bar{D} \nabla \bar{c}) = \nabla \cdot (\alpha_c^{FTab}(\bar{c}, \Delta) \bar{\rho} \bar{D} \nabla \bar{c}) \quad (41)$$

$$\bar{\omega}_c = \Xi \bar{\omega}_c^{FTab}(\bar{c}, \Delta) \quad (42)$$

where the superscript  $FTab$  denotes quantities extracted from one-dimensional filtered laminar pre-mixed flames and tabulated as function of the mass-weighted filtered progress variable  $\bar{c}$  and the filter size  $\Delta$ . Unresolved transport and filtered diffusion fluxes are also modeled from one-dimensional laminar flames. As both transport and reaction terms are multiplied by the wrinkling factor  $\Xi$ , such a model predicts a resolved flame propagating at the turbulent flame burning velocity  $\Xi S_L$ , where  $S_L$  is the laminar flame speed. This model, called F-TACLES (Filtered TABulated Chemistry for Large Eddy Simulations) is found to provide good results, including detailed chemistry features (Fiorina *et al.*, 2010; Auzillon *et al.*, 2011, 2012).

### Artificially thickened flame model

Strictly speaking, the Thickened Flame concept for LES is not a filtered flame model but is linked to this family of models through the method used to close unknown terms in the spatially filtered balance equations. The basic idea, proposed by Butler & O'Rourke (1977); O'Rourke & Bracco (1979) for laminar flame calculations, is to consider a flame thicker than the actual one, but having the same laminar burning velocity  $S_L$ . Following simple theories of laminar premixed flame (Williams, 1985), the burning velocity  $S_L$  and flame thickness  $\delta_L$  may be expressed as:

$$S_L \propto \sqrt{a\bar{\omega}} \quad ; \quad \delta_L \propto \frac{a}{S_L} \quad (43)$$

where  $a$  is the thermal diffusivity and  $\bar{\omega}$  the mean reaction rate. Then, an increase of the flame thickness  $\delta_L$  by

a factor  $\alpha$  while keeping a constant burning velocity  $S_L$  is easily achieved by replacing the thermal diffusivity  $a$  by  $\alpha a$  and the reaction rate  $\bar{w}$  by  $\bar{w}/\alpha$ . If  $\alpha$  is sufficiently large, the thickened flame front may then be resolved on the LES computational mesh.<sup>3</sup> The flame thickening concept was demonstrated in an investigation of combustion instabilities leading to flashback by Thibaut & Candel (1998).

Unfortunately, when the flame is thickened from  $\delta_l$  to  $\alpha\delta_l$ , the interaction between turbulence and chemistry may be modified because the Damköhler number,  $Da = \tau_t/\tau_c$ , comparing turbulent ( $\tau_t$ ) and chemical ( $\tau_c = S_L/\delta_L$ ) time scales is decreased by a factor  $\alpha$ . This point has been investigated using DNS (Colin *et al.*, 2000) and an efficiency function, in fact a flame wrinkling factor  $\Xi$ , has been derived to compensate this effect. In practical applications, the thickened flame approach is implemented by changing the diffusivity and the reaction rate according to Colin *et al.* (2000); Charlette *et al.* (2002a):

$$\begin{aligned} \text{Diffusivity: } & a \longrightarrow \Xi \alpha a \\ \text{Reaction rate: } & W \longrightarrow \Xi W/\alpha \end{aligned}$$

This model is then designed to propagate a flame front of thickness  $\alpha\delta_L$  at the sub-grid scale turbulent burning velocity  $\Xi S_L$ , replacing the flame surface lost in the thickening process by a higher burning velocity.

This approach has been successfully used by Selle *et al.* (2004); Sommerer *et al.* (2004); Durand & Polifke (2007); Freitag *et al.* (2007); Schmitt *et al.* (2007); Boileau *et al.* (2008); Roux *et al.* (2008); Staffelbach *et al.* (2009). Note also that a *dynamic* version<sup>4</sup> of the Thickened Flame Model, where the thickening operation is only applied in the reaction zone to preserve diffusion in non-reacting regions, has also been developed and applied to non-premixed or partially premixed combustion by Légier *et al.* (2002). The thickening factor may also depend on the local grid resolution as in Schmitt *et al.* (2007). Auzillon *et al.* (2011) have compared F-TACLES and TFLES formulations and proposed a relation between filter size  $\Delta$  and thickening factor  $\alpha$  for a given numerical resolution. The flame thickening concept is specifically applicable to premixed flames. It is however less adequate in the non-premixed case because the flame thickness of such flames is essentially controlled by the local strain rate. It is then better to use other schemes as exemplified for example by Schmitt *et al.* (2011) in the case of a non-premixed jet flame, a situation which is typically encountered in liquid rocket engines where reactants are injected separately and form turbulent flames attached to the injection element.

### Flame surface wrinkling and flame surface density modeling

While  $\langle \rho w \rangle_s$  or  $\langle \rho w \rangle_s |\nabla c|$  are extracted from an analysis of one-dimensional flames, it is mandatory to

<sup>3</sup>This property of convection/diffusion/reaction balance equations is easily proved by replacing the spatial coordinate  $x$  by  $x/\alpha$  in the balance equation for a 1D steady propagating flame.

<sup>4</sup>the term *dynamic* is perhaps confusing: it stands for a local adjustment of the thickening factor to act only in the reaction zone but does not correspond to an automatic adjustment of the model parameters from the known resolved scales as is usually implied in LES.

describe the flame / turbulence interactions through a wrinkling factor  $\Xi$  or a flame surface density  $\Sigma$ . These quantities may be deduced from:

- **Algebraic expressions**, such as, for example, Colin *et al.* (2000) or Charlette *et al.* (2002a) expressions or from a fractal analysis. These formulations rely on an equilibrium assumption between flame wrinkling and turbulent fluctuations, which is often not valid for early flame developments.

- **Similarity assumptions**, taking advantage of the knowledge of resolved scales (Knikker *et al.*, 2002).

- **Dynamic modeling** where the model parameters entering algebraic expressions are automatically adjusted during the simulation from the known resolved flow field (Knudsen & Pitsch, 2008; Wang *et al.*, 2011, 2012).

- **Balance equations** for the flame surface density (Boger *et al.*, 1998; Hawkes & Cant, 2000; Richard *et al.*, 2007; Vermorel *et al.*, 2009) or the wrinkling factor,  $\Xi$  (Weller *et al.*, 1998).

### Statistical approach

**Principle** The statistical formalism is based on probability density functions and is first described here for clarity when thermochemical variables  $\varphi$  such as species or temperature depend only on a single variable, for example the mixture fraction  $Z$  for infinitely fast chemistry in non-premixed flames. The Favre filtered fuel mass fraction is defined as (Gao & O'Brien, 1993):

$$\bar{\varphi}(x, t) = \frac{1}{\bar{\rho}} \int_{-\infty}^{+\infty} \rho(x', t) \varphi(Z(x', t)) F(x - x') dx' \quad (44)$$

Introducing the Dirac  $\delta$ -function, this expression becomes:

$$\bar{\varphi}(x, t) = \frac{1}{\bar{\rho}} \int_0^1 \int_{-\infty}^{+\infty} \rho(\Psi) \varphi(\Psi) \delta(Z(x', t) - \Psi) \times F(x - x') dx' d\Psi \quad (45)$$

leading to:

$$\bar{\varphi}(x, t) = \int_0^1 \phi(\Psi) \bar{P}(\Psi, x, t) d\Psi \quad (46)$$

In this expression

$$\bar{P}(\Psi, x, t) = \frac{1}{\bar{\rho}} \int_{-\infty}^{+\infty} \rho(\Psi) \delta(Z(x', t) - \Psi) F(x - x') dx' \quad (47)$$

is the filtered density function (FDF) that may be either presumed or calculated as a solution of a balance equation in a way which is quite similar to what has been implemented in RANS models. This formulation is easily extended to any thermochemical variable. Mass fractions or reaction rates are then determined as:

$$\begin{aligned} \bar{\varphi}(x, t) = & \int_{P_{min}}^{P_{max}} \int_{T_{min}}^{T_{max}} \cdots \int_0^1 \varphi(P, T, Y_1, Y_2, \dots, Y_{n_{sp}}) \\ & \times \bar{P}(P, T, Y_1, Y_2, \dots, Y_{n_{sp}}) dP, dT, dY_1, \dots, dY_{n_{sp}} \end{aligned} \quad (48)$$

When the chemistry is tabulated, the previous expression becomes:

$$\begin{aligned} \bar{\varphi}(x, t) = & \int_{P_{\min}}^{P_{\max}} \int_{T_{\min}}^{T_{\max}} \cdots \int_0^1 \varphi(P, T, \psi_1, \psi_2, \dots, \psi_n) \\ & \times \bar{P}(P, T, \psi_1, \psi_2, \dots, \psi_n) dP, dT, d\psi_1, \dots, d\psi_n \end{aligned} \quad (49)$$

The filtered joint probability  $\bar{P}(\psi_1, \psi_2, \dots, \psi_n)$  describes the sub-grid scale distribution of thermochemical variables  $\psi_i$ , i.e., in the filtering volume centered on location  $x$  at time  $t$ . The challenge is then to determine the filtered density function  $\bar{P}$ .

### Filtered density function (FDF) modeling

The determination of the FDF is quite similar to what has been exploited in RANS formulations:

**Presumed filtered density function** Single variable filtered probability density functions are generally modeled using  $\beta$ -functions, as suggested by Cook & Riley (1994, 1998). These authors also discussed a similarity model to describe the mixture fraction variance without solving an additional balance equation. Olbricht *et al.* (2012) point out that a  $\beta$  distribution is expected for temporal statistics but probably not adapted to instantaneous sub-grid scale distributions, suggesting to retain a top-hat function (uniform probability between minimum and maximum parameter values). Also, Fiorina *et al.* (2010) pointed out that a  $\beta$  distribution does not behave correctly for laminar premixed flames.

Two variables (progress variable and mixture fraction) or multi-variable (adding, for example, strain rate, initial fresh gas temperature, heat losses, exhaust gas recirculation, ... dependencies) filtered probability density functions are modeled assuming statistical independence of parameters. In general, progress variable or mixture fraction distribution are described through  $\beta$ -functions while other parameters are assumed constant at the sub-grid scale level (Dirac functions).

**FDF transport equation** A transport equation for the filtered density function  $\bar{P}(\Psi, x, t)$  may be derived (Gao & O'Brien, 1993) and reads (see for example Haworth, 2011):

$$\begin{aligned} \bar{\rho} \frac{\partial \bar{P}}{\partial t} + \bar{\rho} \tilde{u}_k \frac{\partial \bar{P}}{\partial x_k} = & \underbrace{\frac{\partial}{\partial x_k} \left[ \bar{\rho} \left( \tilde{u}_k - \overline{(u_k | \underline{\varphi} = \underline{\Psi})} \right) \bar{P} \right]}_{\text{Unresolved transport}} \\ & - \underbrace{\bar{\rho} \sum_{i=1}^N \frac{\partial}{\partial \Psi_i} \left[ \left( \frac{1}{\rho} \frac{\partial}{\partial x_k} (\mathcal{J}_{i,k}) \Big|_{\underline{\varphi} = \underline{\Psi}} \right) \bar{P} \right]}_{\text{Molecular diffusion}} \\ & - \underbrace{\bar{\rho} \sum_{i=1}^N \frac{\partial}{\partial \Psi_i} \left( \frac{1}{\rho} \omega_i(\underline{\Psi}) \bar{P} \right)}_{\text{Chemical reaction}} \end{aligned} \quad (50)$$

where  $\overline{(Q | \underline{\varphi} = \underline{\Psi})}$  denotes a conditional averaging of  $Q$  for the sampling values  $\Psi_i$  on the thermochemical variables  $\varphi_i$ .  $\mathcal{J}_{i,k}$  is the  $k^{\text{th}}$  component of the diffusion flux of  $i^{\text{th}}$  thermochemical variable. The LHS terms and the first RHS term correspond to the resolved and unresolved transport in physical space, respectively, while the last two LHS terms describe the FDF evolution in phase (i.e.  $\varphi$ ) space due to molecular diffusion and chemical reaction respectively. Note that the chemical reaction term is closed et need no further modeling. Equation (50) is limited to the composition space (i.e. to the thermochemical variable) but the FDF could also incorporate the velocity components Haworth (2011).

**Comment: CMC modeling** The Conditional Momentum Closure (CMC) approach, primarily proposed by Klimenko (1990) and Bilger (1993), (see also (Klimenko & Bilger, 1999)), is easily extended to LES, writing filtered scalars as:

$$\bar{\varphi}(\underline{x}, t) = \int_0^1 \overline{(\varphi | Z^*; \underline{x}, t)} \bar{P}(Z^*; \underline{x}, t) dZ^* \quad (51)$$

where  $\overline{(\varphi | Z^*; \underline{x}, t)}$  is the filtered conditional mean of  $\varphi$  for a given value  $Z^*$  of the mixture fraction and  $\bar{P}(Z^*; \underline{x}, t)$  is the mass-weighted filtered probability density function of  $Z$ . In Eq. (51),  $\overline{(\varphi | Z^*; \underline{x}, t)}$  describes the filtered chemical flame structure in mixture fraction space and is solution of balance equations. This approach suffers from some drawbacks: it needs a variety of closure schemes, it induces large computational costs (one balance equation per variable  $\phi$  and conditional level  $Z^*$  taken into consideration). It is however conceptually attractive since diffusion flame structures or certain phenomena like autoignition can be directly linked to  $Z$ -iso surfaces (see (Mastorakos *et al.*, 1997)). The CMC approach has been successfully used in some situations (Navarro-Martinez & Kronenburg, 2007, 2009; Triantafyllidis *et al.*, 2009; Garmory & Mastorakos, 2011).

### Mixing approach

The description of reacting flows in terms of turbulent mixing may be based on the extension to LES of simple RANS algebraic models such as the Eddy-Breay-Up or the Eddy-Dissipation-Concept but a more refined formalism has been proposed by Kerstein (1988, 1989, 1990, 1991, 1992): the Linear Eddy Model (LEM), based on a one dimensional stochastic description of turbulent stirring processes. In a LES framework, this analysis is used to represent subgrid scale phenomena.

The **turbulent stirring mechanism** is modeled by a rearrangement process applied to the 1D scalar field. The initial scalar distribution (Fig. 5a) is rearranged on a given segment of size  $l$  according to Fig. 5b ("triplet map"). This process may be viewed as the effect of a single turbulent structure of size  $l$  located in  $x_0$ . Then, the turbulent mixing is simulated from a stochastic description where vortex locations  $x_0$ , vortex sizes  $l$  ( $l_k \leq l \leq \Delta$ , where  $l_k$  is the Kolmogorov length scale

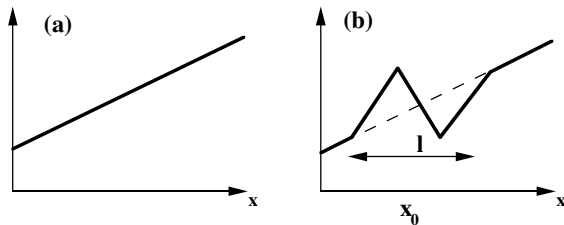


Figure 5. "Triplet map" used in the Linear Eddy Model developed by Kerstein to simulate a one-dimensional turbulent stirring process. (a) before mixing; (b) simulated mixing by a vortex of size  $l$ .

and  $\Delta$  the LES filter size) and vortex frequencies  $\lambda$  are specified according to a given one-dimensional turbulence spectrum.

**Molecular diffusion and chemical processes** are described by one dimensional balance equations:

$$\frac{\partial \rho Y_i}{\partial t} = \frac{\partial}{\partial x} \left( \rho D_i \frac{\partial Y_i}{\partial x} \right) + \dot{\omega}_i \quad (52)$$

In summary, the subgrid scale chemical reaction and turbulent mixing are analyzed on the basis of a one dimensional problem which incorporates a simple stochastic description of turbulence. Any detailed chemistry or diffusion features may be easily included in Eq. (52). This approach also provides a direct estimation of filtered mass fractions  $\bar{Y}_i$  or temperature  $\bar{T}$  without adding additional transport equations for these quantities. Nevertheless, mass fractions and temperature transport between adjacent mesh cells must be modeled. The LEM approach may also be relatively time consuming because a one-dimensional calculation is required in each computational cell.

This approach is probably well suited for large eddy simulations of turbulent mixing (McMurthy *et al.*, 1993) and non premixed combustion, at least when combustion phenomena are essentially controlled by mixing (McMurthy *et al.*, 1992; Menon *et al.*, 1994). It also has been extended to premixed flames (Menon & Kerstein, 1992; Menon *et al.*, 1993). One-Dimensional Turbulence (ODT) concepts have been used in a slightly different manner by Park & Echehki (2012) to cope with turbulent premixed flames.

## Summary

Table 1 summarizes and classifies turbulent combustion models for large eddy simulations in terms of their primary concepts for flame / turbulence interaction and chemical description.

## Comments

**Unresolved scalar fluxes** are generally described from a simple gradient assumption. However, DNS analysis have shown that counter-gradient transport may be observed as in RANS, depending on turbulence levels and heat release rates (Boger *et al.*, 1998). But, as unresolved LES fluxes are smaller than in RANS, model uncertainties are less influential. Since counter-gradient transport may be explained by differential acceleration effects of cold fresh and hot burnt

gases, all characteristic length scales are involved. Thereafter, a portion of the counter-gradient phenomena is directly described in large eddy simulations through resolved motions as shown in Boger & Veynante (2000).

**Dynamic modeling for turbulent combustion**  
LES gives the opportunity to estimate subgrid scale phenomena from known resolved scales. Dynamic models, where model parameters are automatically adjusted during the computations, have been found to effectively describe unresolved momentum or scalar transport a possibility which was pioneered by Germano *et al.* (1991). Up to now, very few attempts have been made to extend the dynamic formalism to reaction rate modeling (Charlette *et al.*, 2002b; Knikker *et al.*, 2004; Knudsen & Pitsch, 2008) perhaps because aerodynamics and combustion behave differently: most of the flow energy is transported by large scale resolved flow motions while combustion is mainly a subgrid scale phenomenon (the flame thickness is generally smaller than the LES grid mesh). However, recent results achieved with dynamic models appear as very promising (Wang *et al.*, 2011, 2012; Veynante *et al.*, 2012; Schmitt *et al.*, 2013).

## EXAMPLES OF TURBULENT COMBUSTION SIMULATIONS

Three examples of practical large eddy simulations including chemistry features are now briefly discussed. The first case corresponds to a well-characterized model scale swirling combustor. This configuration is used to compare several global and reduced kinetic schemes and the results are compared in terms of CO mass fractions. The second case is concerned with the incorporation of heat losses in a tabulated chemistry / filtering flame approach (F-TACLES model). The last case is devoted to MILD (or "flameless") combustion regime where reactants are mixed with burnt gases to reduce flame temperature and the overall nitric oxide emissions.

### Lean partially premixed swirled flame combining reduced/global chemistry and artificially thickened flame model

An interesting configuration for model validation in practical combustion system is the PRECCINSTA swirled burner experimentally investigated by Meier *et al.* (2007). The geometry, shown in Fig. 6, is representative to a certain extent of an actual aeronautical combustion device. It comprises a plenum, a swirl-injector and a combustion chamber. Details on the burner geometry as well as available measurements (velocity, temperature and major species mass fractions) are given in Meier *et al.* (2007). This well-characterized configuration is a target test case for modeling strategies adapted to practical combustors. Roux *et al.* (2005) first performed simulations combining the thickened flame model with a two-step chemical mechanism. Moureau *et al.* (2007) validated a new level-set algorithm to track the flame front position in this configuration. Galpin *et al.* (2008b) coupled a thermo-chemical look-up table with the filtered flow equations through a presumed  $\beta$ -FDF. This configuration was also retained by Fiorina *et al.* (2010) to validate the F-TACLES

Primary concepts		Chemical description				
		Fast chemistry	Single step chemistry	Tabulated chemistry	Reduced schemes	Detailed chemistry
Flame / turbulence	Flame surface	- Level set - Boger <i>et al.</i> - Fractal - FSD Eq.	- TFLES - Duwig	- TFLES-FPI - F-TACLES	-TFLES	
	Statistics	- Presumed pdf	- Presumed pdf	- PCM-FPI - ADF-PCM	- Transp. pdf - CMC	- Transp. pdf - CMC
	Mixing	- EDU / EDC	- EDC - LEM	- LEM	- LEM	- LEM

Table 1. Summary and classification of LES models for reacting flows, in terms of flame / turbulence interaction and chemical descriptions. This classification is based on primary concepts as models may combined several approaches (for example, mixture fraction probability density functions are introduced in flame surface concepts to described partially premixed combustion). The description of the tabulated ADF-PCM model is beyond the scope of this paper but may be found in Michel *et al.* (2009).

model described previously.

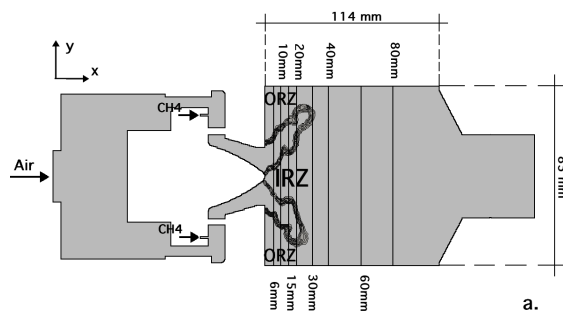


Figure 6. Visualization of the experimental PREC-CINSTA burner (Meier *et al.*, 2007)

Recent results presented by Franzelli *et al.* (2013b) provide a nice illustration of the importance of the chemical modeling on the mean turbulent flame structure. In this numerical study, dry air and pure methane are separately injected at ambient temperature ( $T_f = 320$  K) with air and methane mass flow rates set to  $\dot{m}_{air} = 734.2$  g/min and  $\dot{m}_{CH_4} = 35.9$  g/min, respectively (stable operating point with a global equivalence ratio  $\phi = 0.83$ ). The turbulence / chemistry interaction is represented by the thickened flame model, TFLES. Six chemical mechanisms for methane/air flames, with increasing complexity, are tested: the two-step fitted schemes 2S-CH4.BFER and 2S-CH4.BFER\* (adjusted to account for strain rate effects) developed by Franzelli *et al.* (2010) the four-step fitted (Jones & Lindstedt, 1988) mechanism (referred here as JONES), and the analytical schemes PETERS (Peters, 1985), SESHADRI (Seshadri & Peters, 1989; Chen & Dibble, 1991) and LU (Lu & Law, 2008). The more detailed LU mechanism is used as the reference and the corre-

sponding temperature field in the vertical mid-plane is compared to experimental data in Fig.7.a. Figures 7.b-7.f compare results from the LU mechanism with those using the five other schemes. Although the overall agreement is acceptable, non-negligible differences are observed between chemical models. The consumption speed is overestimated by 2S-CH4.BFER and JONES mechanisms, leading to shorter flames than in the experiment. The modified 2S-CH4.BFER\* scheme, capturing the impact of strain rates, predicts a longer flame than the 2S-CH4.BFER mechanism while the analytical schemes (PETERS, SESHADRI) correctly retrieve the flame length.

Figures 8 compare predicted mean and fluctuating CO mass fraction profiles to experimental data (note that experimental uncertainties on CO was estimated to be of the order of 50%). For the sake of clarity, 2S-CH4.BFER, 2S-CH4.BFER\* and JONES results are displayed at the top in black while the analytical schemes (PETERS and SESHADRI) are shown at the bottom in grey. The simplest 2S-CH4.BFER and 2S-CH4.BFER\* schemes notably underestimate CO mass fractions in the reaction zone but recover the correct level at equilibrium ( $h = 60$  mm). In contrast, the JONES mechanism overestimates maximum values of mean and fluctuating CO mass fractions in the reaction zone as expected from the laminar analysis. Only the analytical schemes (PETERS, SESHADRI) provide fair predictions of CO mass fractions.

### Simulation of a turbulent stratified flame stabilized by heat losses combining premixed flamelet tabulated chemistry and flame filtering

Relevant predictions of the stabilization mechanism of stratified flames requires the accurate modeling of the impact of unsteady mixing processes on the flame structure. Auzillon *et al.* (2011) combined

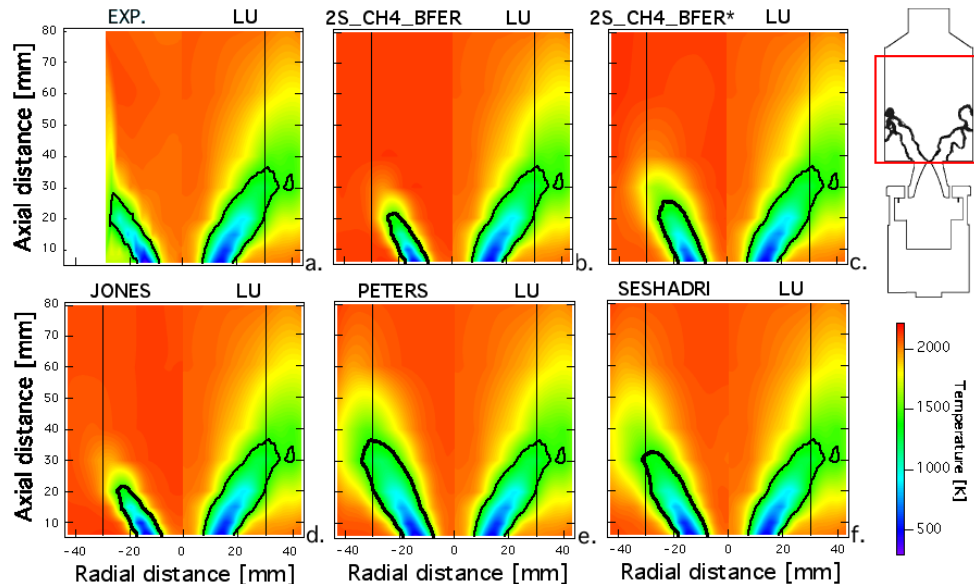


Figure 7. Mean temperature field in the vertical mid-plane. a) Comparison between experiments and LU kinetic scheme. b-f) Comparison between reduced schemes and reference LU kinetic scheme. The black iso-line of progress variable  $c = 0.65$  represents the mean flame surface position.

premixed flamelet tabulated chemistry with flame filtering leading to the F-TACLES (Filtered Tabulated Chemistry for LES) introduced in previous sections. This model was successfully applied to an adiabatic swirled turbulent stratified flame experimentally investigated by Janus *et al.* (2004a,b, 2007).

Flame stabilization mechanisms are more complex in other situations such as jet flames because reactive zones develop close to the burner lips and are affected by heat losses to the walls and injector lips. Roux & Pitsch (2010) and Kuenne *et al.* (2012) suggested that this phenomenon is of importance in the TSF (Turbulent Stratified Flame) configuration designed for turbulent lean premixed or stratified jet flames at high Reynolds number (Böhm *et al.*, 2011; Seffrin *et al.*, 2010). The methane-air generic burner consists of three concentric tubes placed in an air co-flow. Burnt gases, delivered by the central channel to stabilize the flame, are surrounded by two methane air streams with variable equivalence ratios. A RANS 2D-axisymmetric non-reactive computation of the fluid flow inside the burner including conductive heat transfer within the burner walls (between pilot and slot 1) has been conducted with a commercial software. Results show that the pilot stream is cooled by the burner walls and therefore injected below the adiabatic conditions.

To capture the turbulent flame stabilization process, Mercier *et al.* (2013) introduce the influence of heat losses in a premixed flamelet based chemical database, leading to a non-adiabatic correction in the F-TACLES formulation. Numerical simulations of the TSF flame with adiabatic and non-adiabatic F-TACLES formulations have been performed using the low-Mach number code YALES2 (Moureau *et al.*, 2011b). Mean adiabatic temperature and  $\text{CO}_2$  mass fraction are compared to experimental data in Fig. 9 at four axial distances from the pilot tube exit ( $z = 5, 15, 50$  and  $75$  mm). Compared to experimental data, a shift of the flame front prediction is observed with the adiabatic LES. At locations  $z = 5$  mm and  $z = 15$  mm, the numerical

simulation overestimates the measured temperature of the jet by approximately 400 K to 600 K. This significant gap evidences that the pilot stream is cooled by the burner walls and therefore injected below the adiabatic temperature. This gap is closely linked to heat exchanges within the pilot tube. As stated earlier, the inner pilot tube boundary layer is cooled by the wall, decreasing the injected burnt gas enthalpy. Figure 9 shows that the non-adiabatic LES recovers both mean temperature near the burner exit and mean flame position.

Because of heat losses, the flame burning velocity at the pilot tube exit is reduced resulting in a slight shift of the mean flame front position downstream. This phenomenon has been observed in the experiment by direct visualization and its effect on instantaneous flame surface is shown in Fig. 10, displaying an isosurface of filtered progress variable reaction rate colored by local mixture fraction.

### Simulation of a MILD combustor combining chemistry tabulated from non-premixed flamelets and presumed FDF

The thermal efficiency of combustion systems can be increased by transferring heat from exhaust products to fresh gases by means of regenerative heating. Unfortunately, the increase of the reactant temperature tends to promote the nitric oxide ( $\text{NO}_x$ ) formation. A solution to control and reduce peak flame temperature is to operate the burner in the MILD (Moderate or Intense Low-oxygen Dilution) combustion regime (Cavaliere & de Joannon, 2004). A major issue to model MILD combustion is the pronounced sensitivity of the flame structure to the reaction chemistry.

These issues are illustrated by examining the configuration designed and experimented by Castela *et al.* (2012). A reversed flow combustion chamber, where inlet and exhaust ports are located on the same side, ensures sufficiently large residence times to complete

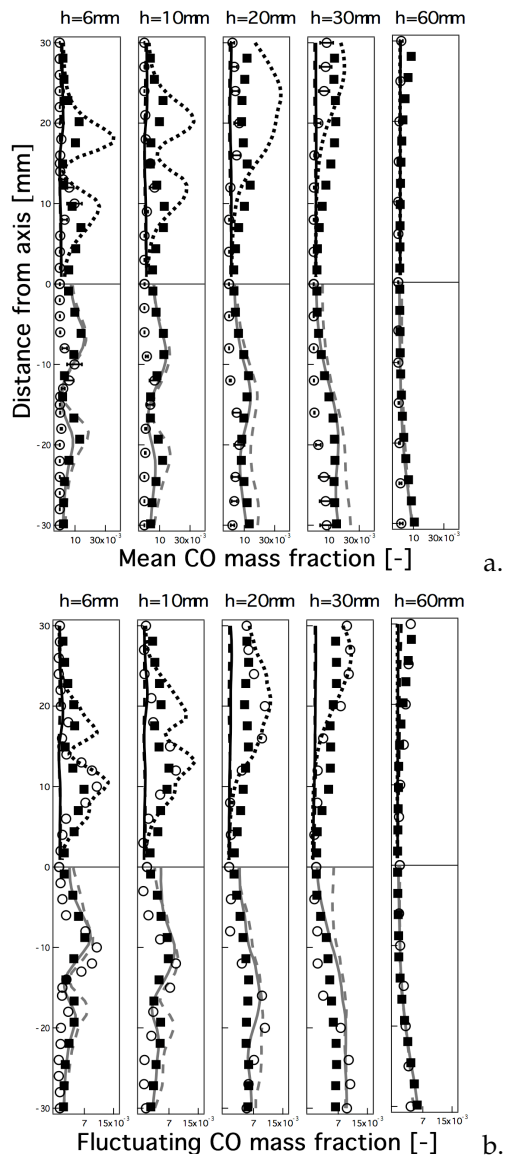


Figure 8. a) Mean and b) fluctuating CO mass fraction profiles at five sections in the chamber. The experimental (○) and LU (■) results are compared to numerical results Top: 2S.CH4.BFER (solid), 2S.CH4.BFER\* (dashed) and JONES (dotted); bottom: PETERS (line) and SESHADRI (dashed).

combustion and promote intense mixing of burned gases with reactants. The injection system combines a central natural gas injection (4 mm diameter) and a surrounding annular jet for preheated (600 K) air.

Assuming *a priori* a non premixed flame structure, Lamouroux *et al.* (2013) tabulated the chemistry from diffusion flamelet trajectories. Three chemistry tabulation techniques presented previously, Steady Strained Flamelet Model (S-SFM), Steady-Flamelet Progress Variable (S-FPV) and Diluted Flamelet Progress Variable (D-FPV), are considered. A statistical description is retained for combustion / turbulence interaction. A  $\beta$ -PDF models mixture fraction statistics while Dirac  $\delta$ -functions are chosen to represent the other chemical look-up table coordinate distributions. The three modeling strategies have been implemented in the finite-volume low Mach number code YALES2 (Moureau

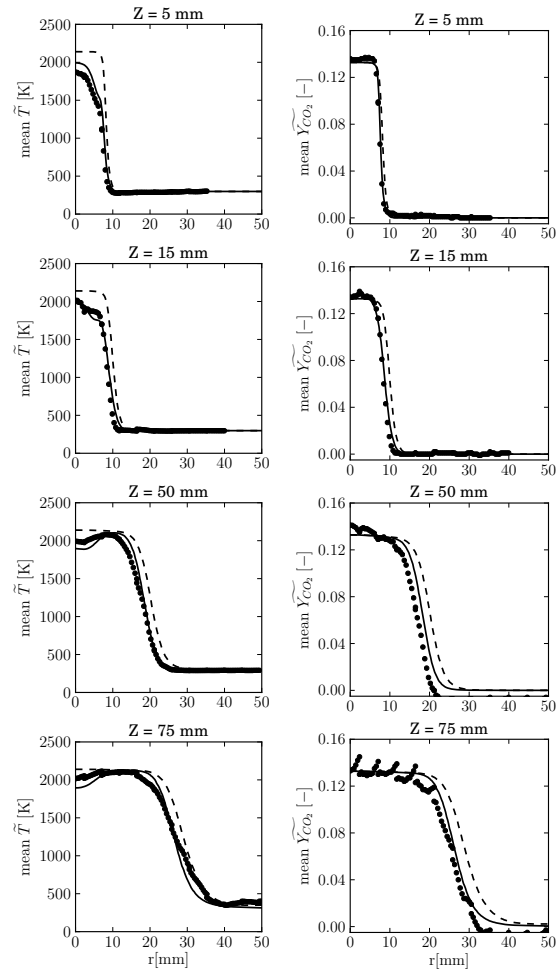


Figure 9. Mean temperature and CO<sub>2</sub> mass fraction at four distances  $z$  from the pilot tube exit ( $z = 0$  mm). -- adiabatic and — non-adiabatic simulations; •• TSF-A-r measurements.

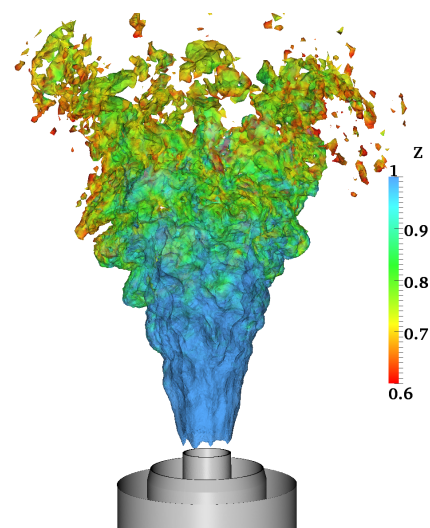


Figure 10. Instantaneous isosurface of filtered reaction rate  $\bar{\rho}\bar{\omega}_{Y_c} = 10 \text{ kg}\cdot\text{s}^{-1}\cdot\text{m}^{-3}$  colored by filtered mixture fraction  $\bar{Z}$  for the non-adiabatic LES.

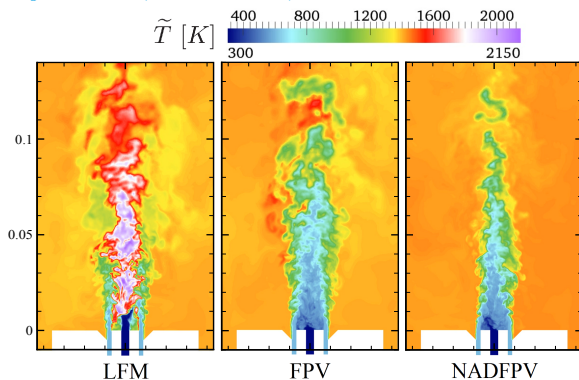


Figure 11. Temperature fields in a median plan for the three models. The distribution is focussed on the injection system and the space scale is given in meters. *left*: LFM model; *middle*: FPV model; *right*: DFPV model.

*et al.*, 2011b). Details on models and numerical simulations are given in Lamouroux *et al.* (2013).

Instantaneous temperature fields are compared in Fig. 11. S-LFM predicts considerably higher temperatures than the other two models. As S-LFM excludes flame extinction, the maximum temperature is close to the adiabatic temperature of 2150 K. The FPV approach allows the existence of unburned mixtures as solutions of the flamelet equations. It therefore predicts a lower maximum temperature. (Fig. 11, middle). The DPSV model (Fig. 11, right), exhibits qualitative similarities with the temperature field predicted by the FPV-model. However, the detachment of the reaction zone from the region between air and fuel inlets as well as the lower temperature field, compared to the two other simulations, is clearly evident. Because of the effect of dilution on the combustion process, the penetration length of the reactants is lower in the DFPV model than in the FPV model.

Time-averaged temperature profiles along the burner centerline are compared in Fig. 12 (top). The LFM model overestimated temperatures until 170 mm. The FPV model predicts a lower heat-release rate in the nozzle near-field, and good agreement with experimental data is obtained for  $x > 150$  mm, corresponding to  $\sim 44$  % of the total length of the combustion chamber. A noticeable improvement is obtained with the DFPV model which reproduces the temperature homogeneity in a better way. Figure 12 (bottom) compares averaged carbon monoxide mole fractions along the centerline. Large differences are observed between the three model predictions. The LFM model predicts a fast chemistry for all equivalence ratios, which leads to a rapid increase of CO in the nozzle-near region, followed by a rapid consumption of CO due to the relaxation towards equilibrium. The delayed combustion process predicted by the FPV model yields to an over-prediction of CO, since the chemistry does not include specificities in chemical reactions due to the mixing with hot burned gases. In contrast, when the dilution of reactants is taken into account, the model qualitatively captures the trend and the magnitude of the experimentally reported CO-profiles.

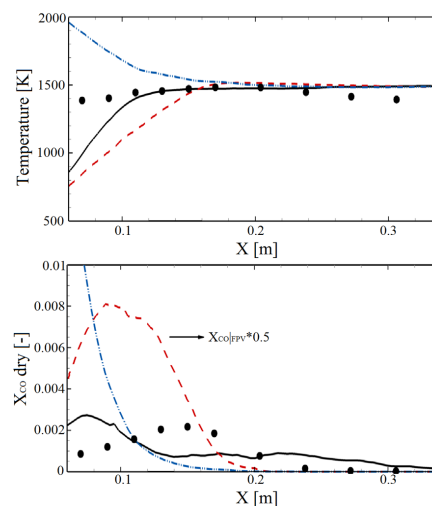


Figure 12. Time-averaged temperature (top) and dry mole fractions of CO (bottom) along the centerline of the configuration. *symbols*: experimental data points; *continuous line*: DFPV model; *dashed line*: FPV model; *dashed-dot-dot line*: LFM model.

## CONCLUSION

The problem of turbulent combustion has posed an essential challenge to scientists working in this field but substantial progress has been accomplished with the development of numerical simulation. Much progress results from a better understanding of the fundamental processes in combination with improved models and advanced numerical simulation tools. Advances in computational performance and the availability of large scale computer power have allowed a rapid development of large eddy simulation of combustion. One may even consider that this has allowed the development of computational flame dynamics which accounts for the interactions between the turbulent flow and the flame. Large eddy simulation constitutes a considerable improvement with respect to the more standard Reynolds Averaged Navier-Stokes (RANS) equations which has prevailed for many years and is still widely used in engineering applications. LES is specifically useful in combustion because it yields a realistic description of the flame on a large scale, provides the spatial location of fresh and burnt gases and naturally contains the history of the flow from the injector to the exhaust. These features are extremely useful when one wishes to analyze dynamical phenomena like ignition, propagation, lean blow out or instabilities. One central issue which constitutes the focal point of this review is that of the interaction between the detailed chemistry and the turbulent flow field. It is not possible to use a full kinetic scheme in such large scale calculations because this would require to solve an excessively large number of equations describing the intermediate species involved. The direct integration of these equations would also not provide a suitable account of the interactions with turbulence. There are better ways to deal with this problem as explained in this article. One method which has been found to be practical and suitable relies on tabulation. Many problems can be treated in this manner.

August 28 - 30, 2013 Poitiers, France

There are however problems when one has to deal with kinetics characterized by slow times which are typical of pollutant formation and destruction in flames like NO<sub>x</sub> or soot. Tabulation methods also rely on specific flame models which are less easy to define in some of the more complex injection configurations found in practice. Such difficulties may be tackled by making use of multiple tables in combination with a method of table selection. It is also possible but more time consuming to rely on in situ flame calculations. On a more general level it is important to be conscious of the uncertainties remaining in this field and to work on the many pending issues.

## Acknowledgments

It is a pleasure to acknowledge many helpful discussions with Nasser Darabiha, Olivier Gicquel, Thomas Schmitt and Ronan Viquelin and to thank Benedetta Franzelli, Pierre Auzillon and Jean Lamouroux for some of the material included in this article.

## REFERENCES

- Auzillon, P., Fiorina, B., Vicquelin, R., Darabiha, N., Gicquel, O. & Veynante, D. 2011 Modeling chemical flame structure and combustion dynamics in LES. *Proc. Combust. Inst.* **33** (1), 1331–1338.
- Auzillon, P., Gicquel, O., Darabiha, N., Veynante, D. & Fiorina, B. 2012 A filtered tabulated chemistry model for LES of stratified flames. *Combust. Flame* **159** (8), 2704 – 2717.
- Baritaud, T., Duclos, J.M. & Fusco, A. 1996 Modeling turbulent combustion and pollutant formation in stratified charge si engines. *Proceedings of the Combustion Institute* **26**, 2627–2635.
- Bell, J. B., ab I. G. Shepherd, M. S. Day, Johnson, M. R., Cheng, R. K., Grcar, J. F., Beckner, V. E. & Lijewski, M. J. 2005 Numerical simulation of laboratory-scale turbulent v-flame. *PNAS* **102**, 10006–10011.
- Bilger, R.W. 1993 Conditional moment closure for turbulent reacting flow. *Phys. Fluids A* **5** (2), 436–444.
- Bockhorn, H., Hbisreuther, P. & Hettel, M. 2009 Numerical modelling of technical combustion. In *100 volumes of "Notes on numerical fluid mechanics"* (ed. E. H. Hirschel & E. Krause), *Notes on numerical fluid mechanics* 100, pp. 325–340. Berlin, Heidelberg: Springer.
- Boger, M. & Veynante, D. 2000 Large eddy simulations of a turbulent premixed V-shape flame. In *Eighth European Turbulence Conference*. Barcelona, Spain.
- Boger, M., Veynante, D., Boughanem, H. & Trouvé, A. 1998 Direct numerical simulation analysis of flame surface density concept for large eddy simulation of turbulent premixed combustion. *Proc. Comb. Inst.* **27**, 917 – 925.
- Böhm, Benjamin, Frank, J. H. & Dreizler, Andreas 2011 Temperature and mixing field measurements in stratified lean premixed turbulent flames. *Proceedings of the Combustion Institute* **33** (1), 1583–1590.
- Boileau, M., Staffellbach, G., Cuenot, B., Poinso, T. & Bérat, C. 2008 LES of an ignition sequence in a gas turbine engine. *Combust. Flame* **154** (1-2), 2 – 22.
- Borghini, R. 1988 Turbulent combustion modelling. *Progress in Energy and Combustion Science* **14** (4), 245–292.
- Boudier, P., Henriot, S., Poinso, T. & Baritaud, T. 1992 A model for turbulent flame ignition and propagation in spark ignition engines. *Proceedings of the Combustion Institute* **24**, 503–510.
- Bradley, D., Gaskell, P. H. & Gu, X. J. 1998 The mathematical modelling of liftoff and blowoff of turbulent non-premixed methane jet flames at high strain rate. In *The Proceedings of the Twenty-Seventh Symposium (Int.) on combustion*, pp. 1199–1206. The Combustion Institute, Pittsburgh.
- Bradley, D., Kwa, L. K., Lau, A. K. C. & Missaghi, M. 1988 Laminar flamelet modelling of recirculating premixed methane and propane-air combustion. *Combust. Flame* **71**, 109–122.
- Butler, T.D. & O'Rourke, P.J. 1977 A numerical method for two-dimensional unsteady reacting flows. *Proc of the Comb. Institute* **16**, 1503 – 1515.
- Bykov, V. & Maas, U. 2007 The extension of the ILDM concept to reaction-diffusion manifolds. *Comb. Th. Modelling* **11** (6), 839–862.
- Bykov, V. & Maas, U. 2009 Problem adapted reduced models based on Reaction-Diffusion Manifolds (REDIMs). *Proc. Comb. Ins.* **32** (Part 1), 561–568.
- Candel, S., Veynante, D., Lacas, F., Maistret, E., Darabiha, N. & Poinso, T. 1990 Coherent flame model: applications and recent extensions. In *Advances in combustion modeling. Series on advances in mathematics for applied sciences* (ed. B. Ed. Larroutou), pp. 19–64. World Scientific, Singapore.
- Candel, S. M. & Poinso, T. 1990 Flame stretch and the balance equation for the flame surface area. *Combustion Science and Technology* **70**, 1–15.
- Castela, M., Veríssimo, A. S., Rocha, A. M. A. & Costa, M. 2012 Experimental study of the combustion regimes occurring in a laboratory combustor. *Combustion Science and Technology* **184** (2), 243–258.
- Cavaliere, A. & de Joannon, M. 2004 Mild combustion. *Progress in Energy and Combustion Science* **30** (4), 329–366.
- Charlette, F., Meneveau, C. & Veynante, D. 2002a A power-law flame wrinkling model for LES of premixed turbulent combustion. Part I: Non-dynamic formulation and initial tests. *Combust. Flame* **131** (1/2), 159 – 180.
- Charlette, F., Meneveau, C. & Veynante, D. 2002b A power-law flame wrinkling model for LES of premixed turbulent combustion. Part II: Dynamic formulation. *Combust. Flame* **131** (1/2), 181 – 197.
- Chen, J. Y. & Dibble, R. W. 1991 *Applications of reduced chemical mechanisms for the prediction of turbulent nonpremixed methane jet flames*, vol. 384 193-226. Springer-Verlag, New York.
- Colin, O., Benkenida, A. & Angelberger, C. 2003 3d modelling of mixing, ignition and combustion phenomena in highly stratified gasoline engines. *Oil and Gas Science and Technology* **58**, 47–62.
- Colin, O., Pires da Cru, A. & Jay, S. 2005 Detailed chemistry-based auto-ignition model including low temperature phenomena applied to 3-D engine calculations. *Proc. Comb. Inst.* **30** (2), 2649 – 2656.
- Colin, O., Ducros, F., Veynante, D. & Poinso, T. 2000 A thickened flame model for large eddy simulations of turbulent premixed combustion. *Phys. Fluids A*

August 28 - 30, 2013 Poitiers, France

- 12 (7), 1843 – 1863.
- Colin, O. & Truffin, K. 2010 A spark ignition model for large eddy simulation based on an fsd transport equation (issim-les). *Proceedings of the Combustion Institute* **33**, 3097–3104.
- Cook, A.W. & Riley, J.J. 1994 A subgrid model for equilibrium chemistry in turbulent flows. *Phys. Fluids A* **6** (8), 2868 – 2870.
- Cook, A.W. & Riley, J.J. 1998 Subgrid scale modeling for turbulent reacting flows. *Combust. Flame* **112**, 593 – 606.
- Dagaut, P. & Cathonnet, M. 2006 The ignition, oxidation and combustion of kerosene : A review of experimental and kinetic modeling. *Progress in Energy and Combustion Science* **32**, 48–92.
- Dahms, R., Peters, N., Stanton, D. W., Tan, Z. & Ewald, J. 2008 Pollutant formation modelling in natural gas SI engines using a level set based flamelet model. *Int. J. Engine Research* **9** (1), 1–14.
- Darabiha, N., Giovangigli, V., Trouvé, A., Candel, S. M. & Esposito, E. 1989 Coherent flame model of turbulent premixed ducted flames. In *Turbulent reactive flows* (ed. R. Borghi & S. N. B. Murthy), pp. 591–637. New York: Springer Verlag.
- Durand, L. & Polifke, W. 2007 Implementation of the thickened flame model for large eddy simulation of turbulent premixed combustion in a commercial solver. In *Proc. ASME Turbo Expo*, , vol. 2, pp. 869 – 878.
- Duwig, C. 2007 Study of a filtered flamelet formulation for large eddy simulation of premixed turbulent flames. *Flow, Turbulence and Combustion* **79** (4), 433–454.
- Embouazza, M. 2005 Etude de l'auto-allumage par réduction des schémas cinétiques chimiques. application à la combustion homogène diesel. PhD thesis, Ecole Centrale Paris.
- Fiorina, B., Baron, R., Gicquel, O., Thévenin, D., Carpentier, S. & Darabiha, N. 2003 Modelling non-adiabatic partially-premixed flames using flame prolongation of ildm. *Combust. Theor. Modell.* **7**, 449–470.
- Fiorina, B., Gicquel, O., Vervisch, L., Carpentier, S. & Darabiha, N. 2005 Approximating the chemical structure of partially-premixed and diffusion counterflow flames using fpi flamelet tabulation. *Combust. Flame* **140** (3), 147–160.
- Fiorina, B., Gicquel, O. & Veynante, D. 2009 Turbulent flame simulation taking advantage of tabulated chemistry self-similar properties. *Proc. Combust. Inst.* **32** (2), 1687–1694.
- Fiorina, B., Vicquelin, R., Auzillon, P., Darabiha, N., Gicquel, O. & Veynante, D. 2010 A filtered tabulated chemistry model for LES of premixed combustion. *Combust. Flame* **157**, 465–475.
- Flemming, F., Sadiki, A. & Janicka, J. 2005 LES using artificial neural network for chemistry representation. *Progress in computational fluid dynamics* **5** (7), 375–385.
- Franzelli, B., Fiorina, B. & Darabiha, N. 2013a A tabulated chemistry method for spray combustion. *Proc. Combust. Inst.* **34**, 1659–1666.
- Franzelli, B., Riber, E. & Cuenot, B. 2013b Impact of the chemical description on a large eddy simulation of a lean partially premixed swirled flame. *Comptes Rendus Mécanique* **341** (1–2), 247 – 256.
- Franzelli, B., Riber, E., Sanjosé, M. & Poinso, T. 2010 A two-step chemical scheme for kerosene-air premixed flames. *Combustion and Flame* **157** (7), 1364 – 1373.
- Freitag, M., Lacor, C., Sadiki, A. & Janicka, J. 2007 Investigation of subgrid scale wrinkling models and their impact on the artificially thickened flame model in large eddy simulations. In *Complex Effects in Large Eddy Simulations* (ed. SC Kassinos, CA Langer, G. Iaccarino & P. Moin), *Lecture Notes in Computational Science and Engineering*, vol. 56, pp. 353 – 369. Springer.
- Galpin, J., Angelberger, C., Naudin, A. & Vervisch, L. 2008a Large-eddy simulation of h-2-air auto-ignition using tabulated detailed chemistry. *Journal of Turbulence* **9** (13), 1–21.
- Galpin, J., Naudin, A., Vervisch, L., Angelberger, C., Colin, O. & Domingo, P. 2008b Large-eddy simulation of a fuel-lean premixed turbulent swirl-burner. *Combust. Flame* **155**, 247–266.
- Gao, F. & O'Brien, E.E. 1993 A large-eddy simulation scheme for turbulent reacting flows. *Phys. Fluids A* **5** (6), 1282–1284.
- Garmory, A. & Mastorakos, E. 2011 Capturing localised extinction in sandia flame f with les-cmc. *Proc. Comb. Inst.* **33** (1), 1673 – 1680.
- Germano, M., Piomelli, U., Moin, P. & Cabot, W.H. 1991 A dynamic subgrid-scale eddy viscosity model. *Phys. Fluids A* **3** (7), 1760 – 1765.
- Gicquel, O., Darabiha, N. & Thévenin, D. 2000 Laminar premixed hydrogen / air counterflow flame simulations using flame prolongation of ildm with differential diffusion. *Proc. Combust. Inst.* **28**, 1901–1908.
- Gicquel, O., Thévenin, D., Hilka, M. & Darabiha, N. 1999 Direct numerical simulation of turbulent premixed flames using intrinsic low-dimensional manifolds. *Combust. Theory Modelling* **3**, 479–502.
- Godel, G., Domingo, P. & Vervisch, L. 2009 Tabulation of NOx chemistry for Large-Eddy Simulation of non-premixed turbulent flames. *Proc. Combust. Inst.* **32** (Part 1), 1555–1561.
- Hasse, C. & Peters, N. 2005 A two mixture fraction flamelet model applied to split injections in a DI Diesel engine. *Proc. Combust. Inst.* **30**, 2755–2762.
- Hawkes, E.R. & Cant, S.R. 2000 A flame surface density approach to large eddy simulation of premixed turbulent combustion. *Proc. Comb. Inst.* **28**, 51 – 58.
- Haworth, D.C. 2011 Progress in probability density function methods for turbulent reacting flows. *Prog. Ener. Comb. Sci.* **36** (2), 168–259.
- Helie, J. & Trouvé, A. 2000 A modified coherent flame model to describe flame propagation in mixtures with a variable composition. *Proceedings of the Combustion Institute* **28**, 193–202.
- Ilhme, M., Marsen, A. L. & Pitsch, H. 2007 Generation of optimal artificial neural networks using a pattern search algorithm: Application to approximation of chemical systems. *Journal of Neural Computation* **20**, 1–29.
- Ilhme, M. & Pitsch, H. 2008 Modeling of radiation and nitric oxide formation in turbulent nonpremixed flames using a flamelet/progress variable formulation. *Physics of Fluids* **20** (5), 055110.
- Ilhme, M. & See, Y.C. 2011 LES flamelet modeling of

August 28 - 30, 2013 Poitiers, France

- a three-stream MILD combustor: Analysis of flame sensitivity to scalar inflow conditions. *Proceedings of the Combustion Institute* **33** (1), 1309 – 1317.
- Ihme, M. & See, Y. C. 2010 Large-eddy simulation of a turbulent lifted flame in a vitiated co-flow. *Combust. Flame* **157** (10).
- Ihme, M., Shunn, L. & Zhang, J. 2012 Regularization of reaction progress variable for application to flamelet-based combustion models. *Journal of Computational Physics* **231** (23), 7715 – 7721.
- Janus, B., Dreizler, A. & Janicka, J. 2004a Experimental study on stabilization of lifted swirl flames in a model GT combustor. *Flow Turbul. Combust.* (75), 293 – 315.
- Janus, B., Dreizler, A. & Janicka, J. 2004b Flow field and structure of swirl stabilized non-premixed natural gas flames at elevated pressure. *ASME Turbo Expo, Vienna* pp. 293 – 315.
- Janus, B., Dreizler, A. & Janicka, J. 2007 Experiments on swirl stabilized non-premixed natural gas flames in a model gasturbine combustor. *Proc. Combust. Inst.* **31** (2), 3091 – 3098.
- Jay, S. & Colin, C. 2011 A variable volume approach of tabulated detailed chemistry and its applications to multidimensional engine simulations. *Proc. Comb. Inst.* **33** (2), 3065 – 3072.
- Jones, W. P. & Lindstedt, R. P. 1988 Global reaction schemes for hydrocarbon combustion. *Combust. Flame* **73**, 233–249.
- Kee, R. J., Grcar, J. F., Smooke, M. D. & Miller, J. A. 1985 A fortran program for modelling steady laminar one-dimensional premixed flames. *Tech. Rep. SAND85-8240-UC-401*. Sandia National Laboratories.
- Kerstein, A.R. 1988 A linear eddy model of turbulent scalar transport and mixing. *Comb. Sci. Tech.* **60**, 391.
- Kerstein, A.R. 1989 Linear-Eddy modeling of turbulent transport: Part II. Application to shear layer mixing. *Combust. Flame* **75** (3 - 4), 397 – 413.
- Kerstein, A.R. 1990 Linear-eddy modelling of turbulent transport. Part 3. Mixing and differential molecular diffusion in round jets. *J. Fluid Mech.* **216**, 411 – 435.
- Kerstein, A.R. 1991 Linear-eddy modelling of turbulent transport. Part 6. Microstructure of diffusive scalar mixing fields. *J. Fluid Mech.* **231**, 361 – 394.
- Kerstein, A.R. 1992 Linear eddy modeling of turbulent transport. Part 4: structure of diffusion flames. *Comb. Sci. Tech.* **81**, 75 – 96.
- Kerstein, A.R., Ashurst, W. & Williams, F.A. 1988 Field equation for interface propagation in an unsteady homogeneous flow field. *Physical Review A* **37** (7), 2728–2731.
- Klimenko, A.Y. 1990 Multicomponent diffusion of various admixtures in turbulent flow. *Fluid Dynamics* **25** (3), 327 – 334.
- Klimenko, A.Y. & Bilger, R.W. 1999 Conditional moment closure for turbulent combustion. *Progress in Energy and Combustion Science* **25** (6), 595 – 687.
- Knikker, R., Veynante, D. & Meneveau, C. 2002 A priori testing of a similarity model for large eddy simulations of turbulent premixed combustion. *Proc. Comb. Inst.* **29**, 2105 – 2111.
- Knikker, R., Veynante, D. & Meneveau, C. 2004 A dynamic flame surface density model for large eddy simulation of turbulent premixed combustion. *Phys. Fluids* **16** (11), L91 – L94.
- Knudsen, E., Kim, S. H. & Pitsch, H. 2010 An analysis of premixed flamelet models for large eddy simulation of turbulent combustion. *Phys. Fluids* **22** (11).
- Knudsen, E. & Pitsch, H. 2008 A dynamic model for the turbulent burning velocity for large eddy simulation of premixed combustion. *Combust. Flame* **154**, 740 – 760.
- Kuenne, G., Seffrin, F., Fuest, F., Stahler, T., Ketelheun, A., Geyer, D., Janicka, J. & Dreizler, A. 2012 Experimental and numerical analysis of a lean premixed stratified burner using 1D Raman/Rayleigh scattering and large eddy simulation. *combust. Flame* **159** (2669-2689).
- Lam, S. H. & Goussis, D. A. 1988 Understanding complex chemical kinetics with computational singular perturbation. In *Proceedings of the 22nd Symp. (Int.) on Combustion. The Combustion Institute, Pittsburgh.*, pp. 931–941.
- Lamouroux, J., Ihme, M., Fiorina, B. & Gicquel, O. 2013 Flamelet-progress variable approach for mild combustion regimes. *Submitted*.
- Légier, J.P., Varoquié, B., Lacas, F., Poinso, T. & Veynante, D. 2002 Large eddy simulation of a non-premixed turbulent burner using a dynamically thickened flame model. In *IUTAM Symposium on Turbulent Mixing and Combustion* (ed. A. Pollard & S. Candel), , vol. 70, pp. 315 – 326. Kluwer Academic Publishers.
- Lu, T. & Law, C.K. 2008 A criterion based on computational singular perturbation for the identification of quasi steady state species: A reduced mechanism for methane oxidation with no chemistry. *Combust. Flame* **154** (4), 761–774.
- Maas, U. & Pope, S. 1992 Simplifying chemical kinetics: Intrinsic low-dimensional manifolds in composition space. *Combust. Flame* **88**, 239–264.
- Maragkos, G., Rauwoens, P. & Merci, B. 2013 A new methodology to incorporate differential diffusion in cfd simulations of reactive flows. *Combustion and Flame* **160**, 1903–1905.
- Marble, F. E. & Broadwell, J. E. 1977 The coherent flame model for turbulent chemical reactions. *Tech. Rep. Project Squid Report TRW-9-PU*. TRW.
- Masri, A.R., Bilger, R.W. & Dibble, R.W. 1988 Turbulent non-premixed flames of methane near extinction. *Combust. Flame* **73**, 261–258.
- Mastorakos, E., Baritaud, T.A. & Poinso, T.J. 1997 Numerical simulations of autoignition in turbulent mixing flows. *Combust. Flame* **109**, 198 – 223.
- McMurthy, P.A., Gansauge, T.C., Kerstein, A.R. & Krueger, S.K. 1993 Linear eddy simulations of mixing in a homogeneous turbulent flow. *Phys. Fluids A* **5** (4), 1023 – 1034.
- McMurthy, P.A., Menon, S. & Kerstein, A.R. 1992 A linear eddy subgrid model for turbulent reacting flows: application to hydrogen-air combustion. *Proc. Comb. Inst.* **24**, 271 – 278.
- Meier, W., Weigand, P., Duan, X.R. & Giezendanner-Thoben, R. 2007 Detailed characterization of the dynamics of thermoacoustic pulsations in a lean premixed swirl flame. *Combustion and Flame* **150** (1-2), 2 – 26.
- Menon, S. & Jou, W.H. 1991a Large eddy simulations

August 28 - 30, 2013 Poitiers, France

- of combustion instability in an axisymmetric ramjet combustor. *Combust. Sci. Technol.* **75**, 53–72.
- Menon, S. & Jou, W. H. 1991b Large eddy simulation of combustion instability in an axisymmetric ramjet combustor. *Combustion Science and Technology* **75**, 53–72.
- Menon, S. & Kerstein, A.R. 1992 Stochastic simulation of the structure and propagation rate of turbulent premixed flames. *Proc. Comb. Inst.* **24**, 443 – 450.
- Menon, S., McMurthy, P.A. & Kerstein, A.R. 1993 A linear eddy mixing model for large eddy simulation of turbulent combustion. In *Large eddy simulation of complex engineering and geophysical flows* (ed. B. Galperin & S.A. Orzag), pp. 87 – 314. Cambridge University Press.
- Menon, S., McMurthy, P.A., Kerstein, A.R. & Chen, J.Y. 1994 Prediction of NO<sub>x</sub> production in a turbulent hydrogen-air jet flame. *J. Propul. Power* **10**, 161–168.
- Mercier, R., Auzillon, P., Moureau, V., Darabiha, N., Gicquel, O., Veynante, D. & Fiorina, B. 2013 Les modeling of the impact of heat losses and differential diffusion on a turbulent stratified flame. *Submitted*.
- Michel, J.B., Colin, O., Angelberger, C. & Veynante, D. 2009 Using the tabulated diffusion flamelet model ADF-PCM to simulate a lifted methane-air jet flame. *Combust. Flame* **156** (7), 1318–1331.
- Michel, J.B., Colin, O. & Veynante, D. 2008 Modeling ignition and chemical structure of partially premixed turbulent flames using tabulated chemistry. *Combustion and Flame* **152** (1-2), 80–99.
- Mizobuchi, Y., Tachibana, S., Shinjo, J., Ogawa, S. & Takeno, T. 2002 A numerical analysis of the structure of a turbulent hydrogen jet-lifted flame. *Proceedings of the Combustion Institute* **29**, 2009 – 2015.
- Moureau, V., Domingo, P. & Vervisch, L. 2011a Design of a massively parallel cfd code for complex geometries. *Comptes Rendus Mecanique* **339**, 141–148.
- Moureau, V., Domingo, P. & Vervisch, L. 2011b From large-eddy simulation to direct numerical simulation of a lean premixed swirl flame: Filtered laminar flame-pdf **158** (7), 1340–1357.
- Moureau, V., Domingo, P. & Vervisch, L. 2011c From large eddy simulation to direct numerical simulation of a lean premixed swirl flame: filtered laminar flame pdf modeling. *Combust. Flame* **158**, 1340–1357.
- Moureau, V., Fiorina, B. & Pitsch, H. 2009 A level set formulation for premixed combustion LES considering the turbulent flame structure. *Combust. Flame* **156** (4), 801–812.
- Moureau, V., Minot, P., Pitsch, H. & Berat, C. 2007 A ghost-fluid method for large-eddy simulations of premixed combustion in complex geometries. *J. Comput. Phys.* **221** (2), 600 – 614.
- Naudin, A., Fiorina, B., Paubel, X., Veynante, D. & Vervisch, L. 2006 Self-similar behavior of chemistry tabulation in laminar and turbulent multi-fuel injection combustion systems. In *Proceedings of the 2006 Summer Program*. Center For Turbulence Research, Stanford University.
- Navarro-Martinez, S. & Kronenburg, A. 2007 LES-CMC simulations of a turbulent bluff-body flame. *Proc. Comb. Inst.* **31**, 1721–1728.
- Navarro-Martinez, S. & Kronenburg, A. 2009 LES-CMC simulations of a lifted methane flame. *Proc. Comb. Inst.* **32** (1), 1509 – 1516.
- Nguyen, P.D., Vervisch, L., Subramanian, V. & Domingo, P. 2010 Multidimensional flamelet-generated manifolds for partially premixed combustion. *Combust. Flame* **157** (1), 43–61.
- Niu, Y.S., Vervisch, L. & Tao, P.D. 2013 An optimization-based approach to detailed chemistry tabulation: Automated progress variable definition. *Combustion and Flame* **160** (4), 776 – 785.
- van Oijen, J. A. & de Goey, L. P. H. 2009 Predicting no formation with flamelet generated manifolds. *Proceedings of the European Combustion Meeting*.
- van Oijen, J. A., Lammers, F. A. & de Goey, L. P. H. 2001 Modelling of complex premixed burner systems by using flamelet-generated manifolds. *Combust. Flame* **127** (3), 2124–2134.
- Olbricht, C., Stein, O.T., Janicka, J., van Oijen, J.A., Wysocki, S. & Kempf, A.M. 2012 {LES} of lifted flames in a gas turbine model combustor using top-hat filtered {PFGM} chemistry. *Fuel* **96** (0), 100 – 107.
- O'Rourke, P. J. & Bracco, F. V. 1979 Two scaling transformations for the numerical computation of multidimensional unsteady laminar flames. *Journal of Computational Physics* **33**, 185–203.
- Park, J. & Echehki, T. 2012 LES-ODT study of turbulent premixed interacting flames. *Combust. Flame* **159** (2), 609–620.
- Pecquery, F., Moureau, V. & Vervisch, L. 2013 *Submitted to Combust. Flame*.
- Peters, N. 1984 Laminar diffusion flamelet models in non-premixed turbulent combustion. *Prog. Energy Combustion. Sci.* **10**, 319–339.
- Peters, N. 1985 Numerical and asymptotic analysis of systematically reduced reaction schemes for hydrocarbon flames. *Lecture Notes in Physics* **241**, 90–109.
- Peters, N. 1986 Laminar flamelet concepts in turbulent combustion. In *In The Proceedings of the 21rst Symposium (international) on Combustion*, pp. 1231–1250. The Combustion Institute, Pittsburgh.
- Peters, N. 2000 *Turbulent Combustion*. Cambridge University Press.
- Piana, J., Veynante, D., Candel, S. & Poinso, T. 1997 Direct numerical simulation analysis of the g-equation in premixed combustion. In *Direct and Large Eddy Simulation II* (ed. J. P. Chollet, P. R. Voke & L. Kleiser), pp. 321–330. Kluwer Academic Publishers.
- Pierce, C. & Moin, P. 2004 Progress-variable approach for large-eddy simulation of non-premixed turbulent combustion. *Journal of Fluid Mechanics* **504**, pp 73–97.
- Pitsch, H. 2005 A consistent level set formulation for large-eddy simulation of premixed turbulent combustion. *Combust. Flame* **143** (4), 587–598.
- Pitsch, H. 2006 Large eddy simulation of turbulent combustion. *Annual Review of Fluid Mechanics* **38**, 453–482.
- Pitsch, H. 2006 Large-eddy simulation of turbulent combustion. *Annu. Rev. Fluid Mech.* **38**, 453–482.
- Pitsch, H., Desjardins, O., Balarac, G. & Ihme, M. 2008 Large-eddy simulation of turbulent reacting flows. *Progress in Aerospace Sciences* **44** (466-478).
- Pitsch, H. & Duchamp de la Geneste, L. 2002 Large eddy simulation of premixed turbulent combustion using a level-set approach. *Proc. Comb. Institute* **29**, 2001 – 2008.

August 28 - 30, 2013 Poitiers, France

- Pitsch, H. & Peters, N. 1998 A consistent flamelet formulation for non-premixed combustion considering differential diffusion effects. *combust. Flame* **114**, 26–40.
- Poinsot, T. 1996 Using direct numerical simulation to understand turbulent premixed combustion (plenary lecture). *Proceedings of the Combustion Institute* **26**, 219–232.
- Poinsot, T., Candel, S. & Trouvé, A. 1996 Application of direct numerical simulation to premixed turbulent combustion. *Progress in Energy and Combustion Science* **21**, 531–576.
- Poinsot, T. & Lele, S. K. 1992 Boundary conditions for direct simulations of compressible viscous flows. *J. Comput. Phys.* **1** (101), 104–129.
- Poinsot, T. & Veynante, D. 2005 *Theoretical and Numerical Combustion*. R. T. Edwards, Inc.
- Poludnenko, A. Y. & Oran, E. S. 2010 The interaction of high-speed turbulence with flames: Global properties and internal flame structure. *Combust. Flame* **157**, 995–1011.
- Poludnenko, A. Y. & Oran, E. S. 2011 The interaction of high-speed turbulence with flames: Turbulent flame speed. *Combust. Flame* **158**, 301–326.
- Pope, S. B. 1997 Computationally efficient implementation of combustion chemistry using in situ adaptive tabulation. *Combust. Theory Modelling* **1**, 41–63.
- Regele, J.D., Knudsen, E., Pitsch, H. & Blanquart, G. 2013 A two-equation model for non-unity lewis number differential diffusion in lean premixed laminar flames. *Combustion and Flame* **160** (2), 240 – 250.
- Ribert, G., Gicquel, O., Veynante, D. & Darabiha, N. 2006 Tabulation of complex chemistry based on self-similar behavior of laminar premixed flames. *Combust. Flame* **146**, 649–664.
- Richard, S., Colin, O., Vermorel, O., Benkenida, A., Angelberger, C. & Veynante, D. 2007 Towards large eddy simulation of combustion in spark ignition engines. *Proc. Comb. Inst.* **31** (2), 3059 – 3066.
- Roux, A., Gicquel, L.Y.M., Sommerer, Y. & Poinsot, T. 2008 Large eddy simulation of mean and oscillating flow in a side-dump ramjet combustor. *Combust. Flame* **152** (1-2), 154 – 176.
- Roux, A. & Pitsch, H. 2010 Large-eddy simulation of stratified combustion. In *Annual Research Briefs*, pp. 275–289. Center For Turbulence Research.
- Roux, S., Lartigue, G., Poinsot, T., Meier, U. & Berat, C. 2005 Studies of mean and unsteady flow in a swirled combustor using experiments, acoustic analysis, and large eddy simulations. *Combustion and Flame* **141** (1-2), 40 – 54.
- Schmidt, H. & Klein, R. 2003 A generalized level-set/in-cell-reconstruction approach for accelerating turbulent premixed flames. *Comb. Theory and Modelling* **7** (2), 243–267.
- Schmitt, P., Poinsot, T., Schuermans, B. & Geigle, K. 2007 Large-eddy simulation and experimental study of heat transfer, nitric oxide emissions and combustion instability in a swirled turbulent high-pressure burner. *J. Fluid Mech.* **570**, 17–46.
- Schmitt, T., Méry, Y., Boileau, M. & Candel, S. 2011 Large-Eddy Simulation of oxygen/methane flames under transcritical conditions. *Proceedings of the Combustion Institute* **33**, 1383–1390.
- Schmitt, T., Sadiki, A., Fiorina, B. & Veynante, D. 2013 Impact of dynamic wrinkling model on the prediction accuracy using the F-TACLES combustion model in swirling premixed turbulent flames. *Proc. Comb. Inst.* **34** (1), 1261–1268.
- Schneider, E., Maltsev, A., Sadiki, A. & Janicka, J. 2008 Study on the potential of BML-approach and G-equation concept-based models for predicting swirling partially premixed combustion systems: URANS computations. *Combust. Flame* **152** (4), 548–572.
- Seffrin, F., Fuest, F., Geyer, D. & Dreizler, A. 2010 Flow field studies of a new series of turbulent premixed stratified flames. *Combustion and Flame* **157** (2), 384 – 396.
- Selle, L., Lartigue, G., Poinsot, T., Koch, R., Schildmacher, K.U., Krebs, W., Prade, B., Kaufmann, P. & Veynante, D. 2004 Compressible large eddy simulation of turbulent combustion in complex geometry on unstructured meshes. *Combust. Flame* **137**, 489 – 505.
- Seshadri, K. & Peters, N. 1989 In *Workshop on Reduced Kinetic Mechanism and Asymptotic Approximations for Methane-Air Flames*. La Jolla, California.
- Smith, G. P., Golden, D. M., Frenklach, M., Moriarty, N. W., Eiteneer, B., Goldenberg, M., Bowman, C. T., Hanson, R. K., Song, S., Gardiner, W. C., Lissianski, V. V. & Qin, Z. 1999 <http://www.me.berkeley.edu/gri-mech/>.
- Sommerer, Y., Galley, D., Poinsot, T., Ducruix, S., Lacas, F. & Veynante, D. 2004 Simulation and experimental study of flash-back and blow-off in a lean partially premixed swirled burner. *J. Turbulence* **5**.
- Staffelbach, G., Gicquel, L.Y.M., Boudier, G. & Poinsot, T. 2009 Large eddy simulation of self excited azimuthal modes in annular combustors. *Proc. Comb. Inst.* **32**, 2909 – 2916.
- Sutherland, J. C., Smith, P. J. & Chen, J. H. 2005 Quantification of differential diffusion in nonpremixed systems. *Combustion Theory and Modelling* **9** (2), 365–383.
- Thévenin, D. 2005 Three-dimensional direct simulations and structure of expanding turbulent methane flames. *Proceedings of the Combustion Institute* **30**, 629–637.
- Thévenin, D., Gicquel, O., de Charentenay, J., Hilbert, R. & Veynante, D. 2002 Two-versus three-dimensional direct simulations of turbulent methane flame kernels using realistic chemistry. *Proceedings of the Combustion Institute* **29**, 2031–2039.
- Thibaut, D. & Candel, S. 1998 Numerical study of unsteady turbulent premixed combustion. application to flashback simulation. *Combustion and Flame* **113**, 51–65.
- Triantafyllidis, A., Mastorakos, E. & Eggels, R.L.G.M. 2009 Large eddy simulations of forced ignition of a non-premixed bluff-body methane flame with conditional moment closure. *Combust. Flame* **156** (12), 2328 – 2345.
- Trouvé, A., Veynante, D., Bray, K. N. C. & Mantel, T. 1994 The coupling between flame surface dynamics and species mass conservation in premixed turbulent combustion. In *Proceedings of the Summer Program*, pp. 95–124. Center for Turbulence Research, NASA Ames/Stanford Univ.
- Tudorache, D., Auzillon, P., Gicquel, O., Darabiha, N. &



August 28 - 30, 2013 Poitiers, France

- Fiorina, Benoit 2011 Development of a chemical kinetics tabulation method for the prediction of diesel engine pollutants. In *23th ICDERS, Irvine, USA*.
- Vermorel, O., Richard, S., Colin, O., Angelberger, C., Benkenida, A. & Veynante, D. 2009 Towards the understanding of cyclic variability in a spark ignited engine using multi-cycle les. *Combust. Flame* **156** (8), 1525 – 1541.
- Vervisch, L. & Poinso, T. 1998 Direct numerical simulation of non premixed turbulent flames. *Annual Review of Fluid Mechanics* **30**, 655–692.
- Veynante, D., Fiorina, B., Domingo, P. & Vervisch, L. 2008 Using self-similar properties of turbulent premixed flames to downsize chemical tables in high-performance numerical simulations. *Combust. Theory and Modelling* p. In Press.
- Veynante, D., Schmitt, T., Boileau, M. & Moureau, V. 2012 Analysis of dynamic models for turbulent premixed combustion. In *Proceedings of the Summer Program*, pp. 387 – 396. Center for Turbulence Research.
- Veynante, D. & Vervisch, L. 2002 Turbulent combustion modeling. *Progress in Energy and Combustion Science* **28**, 193–266.
- Vicquelin, R. 2010 Tabulation de la cinétique chimique pour la modélisation et la simulation de la combustion turbulente. PhD thesis, Ecole Centrale Paris.
- Vicquelin, R., Fiorina, B., Payet, S., Darabiha, N. & Gicquel, O. 2011 Coupling tabulated chemistry with compressible CFD solvers. *Proc. Combust. Inst.* **33** (1), 1481–1488.
- Wang, G., Boileau, M. & Veynante, D. 2011 Implementation of a dynamic thickened flame model for large eddy simulations of turbulent premixed combustion. *Combust. Flame* **158** (11), 2199–2213.
- Wang, G., Boileau, M., Veynante, D. & Truffin, K. 2012 Large eddy simulation of a growing turbulent premixed flame kernel using a dynamic flame surface density model. *Combust. Flame* **159** (8), 2742 – 2754.
- Wang, P. & Bai, X.S. 2005 Large eddy simulation of turbulent premixed flames using level-set g-equation. *Proc. Comb. Inst.* **30**, 583 – 591.
- Weise, S., Messig, D., Meyer, B. & Hasse, C. 2013 An abstraction layer for efficient memory management of tabulated chemistry and flamelet solutions. *Combust. Theory and Modelling* **17** (3), 411–430.
- Weller, H.G., Tabor, G., Gosman, A.D. & Fureby, C. 1998 Application of a flame-wrinkling LES combustion model to a turbulent mixing layer. *Proc. Comb. Inst.* **27**, 899 – 907.
- Westbrook, C. K., Mizobuchi, Y., Poinso, T., Smith, P. & Warnatz, J. 2005 Computational combustion. *Proceedings of the Combustion Institute* **30**, 125–157.
- Williams, F.E. 1985 *Combustion Theory*, 2nd edn. Addison-Wesley.